Chapter 4

Results and Discussion

4.1 Results of determining the calcining temperature

A PL5T powder of 5 gms was used to study the calcination temperature. X-ray diffraction patterns of PL5T powders calcined for 1 hr at temperature ranging from 300°C to 800°C are shown in fig. 18. Unreacted raw material patterns existed up to 600°C but a single phase of tetragonal structure was detected at 700°C and 800°C.

For heat-treatment of a larger amount of samples, 50 g. PL5T powders were examined at temperature ranging from 750°C to 850°C. Fig 19 shows the X-ray diffraction patterns of PL5T powder (50gms) calcined at 800°C for 1 hr , 750°C and 800°C for 2 hrs. The results showed a single phase for samples. For the calcining temperature of 750°C with a soaking time of 2 hr the diffraction peaks become more sharply defined. Experimentally, the best firing schedule so far was attained when the PL5T compositions (50 gms) were subjected to heat-treatment using a heating rate of 120°C/hr and holding the samples at 750°C for 2 hrs.

The X-ray diffraction patterns of PC5T powder (50gms) calcined in air for 2 hrs at temperature between 750°C to 850°C using a heating rate of 120°C/hr are shown in fig. 20. The results from all samples showed a single phase. Heating all samples for 2 hrs at a temperature of 800°C resulted in a single tetragonal phase exhibiting sharply defined XRD patterns. This firing schedule was also adapted for all PCT compositions studied.

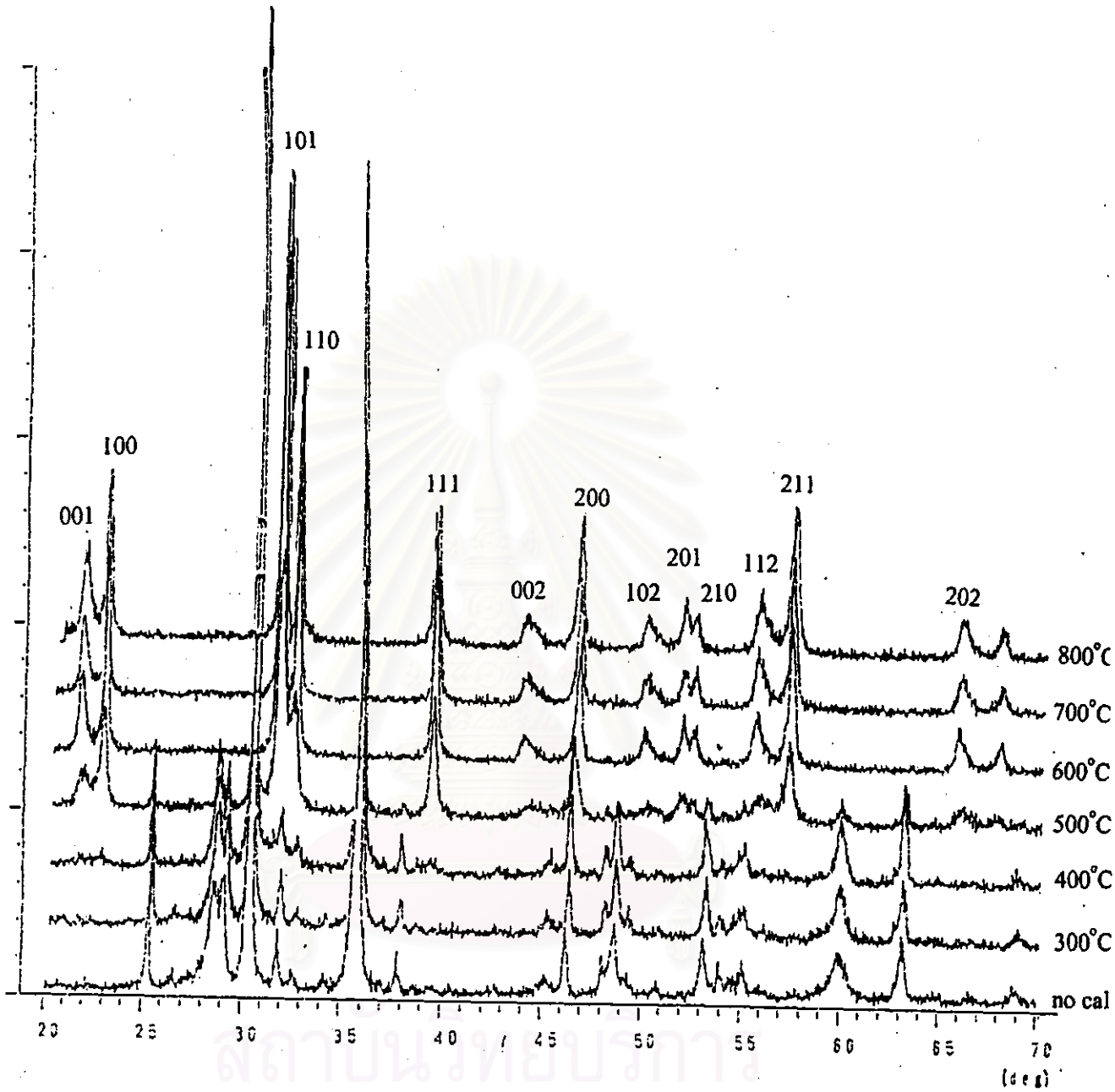

Fig. 18 X-ray diffraction patterns of PL5T (5 gms) powder before and after calcined at 300°C to 800°C for 1 hr.

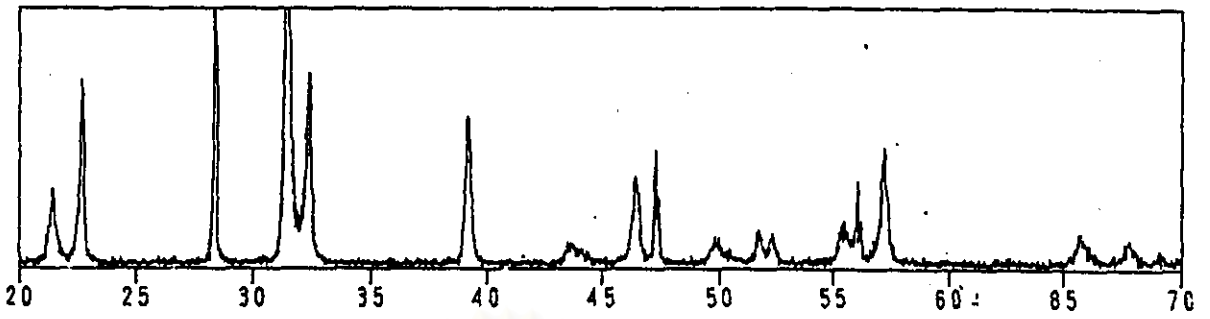

(a)

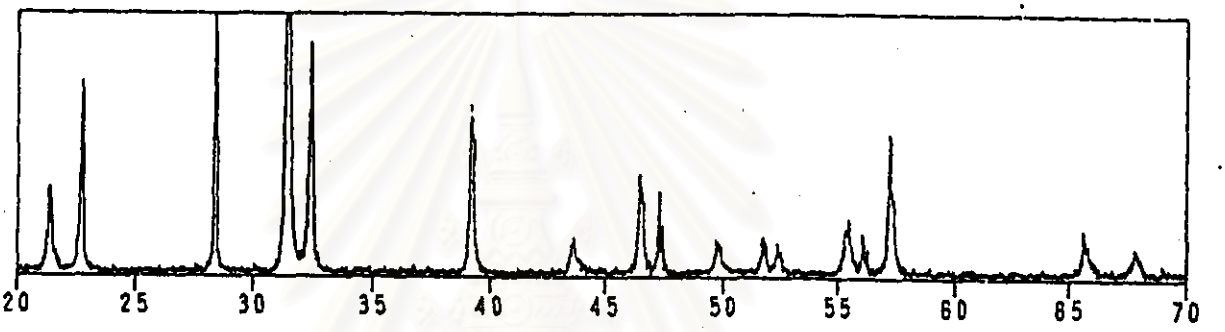

(b)

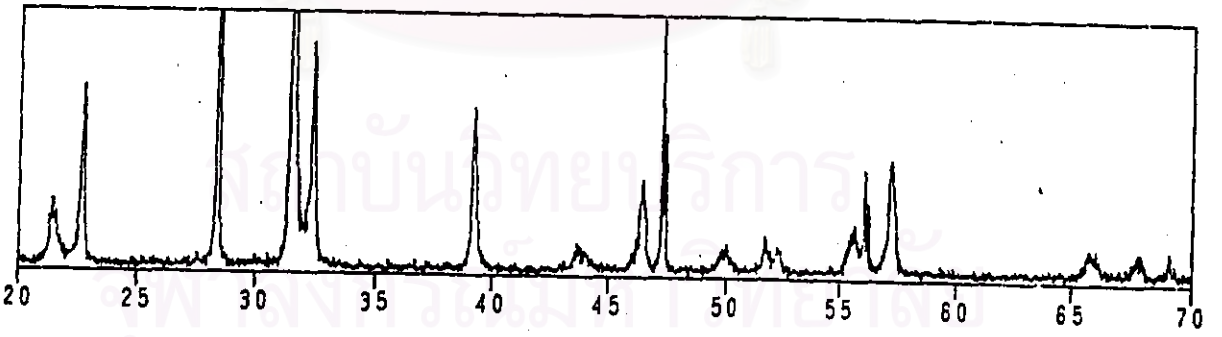

(c)

Fig. 19 The X-ray diffraction patterns of PL5T (50gms) calcined at (a) 750°C for 2 hrs , (b) 800°C for 2 hrs and (c) 800°C for 1 hr.

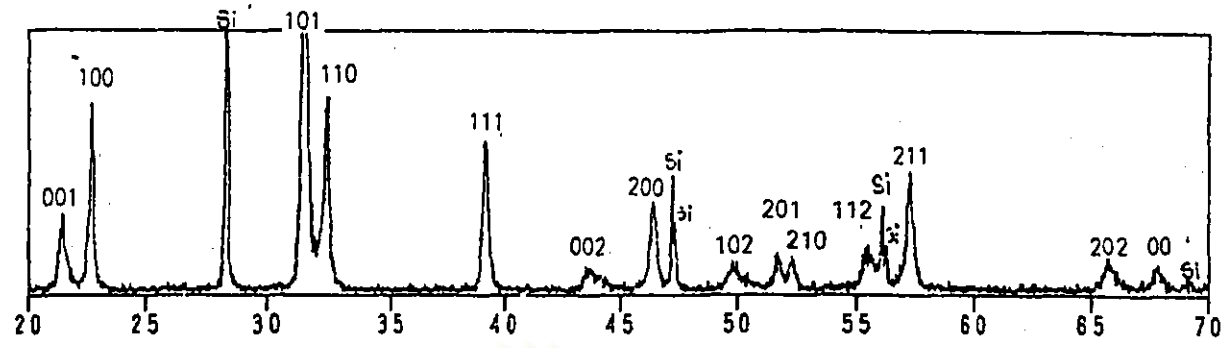

(a)

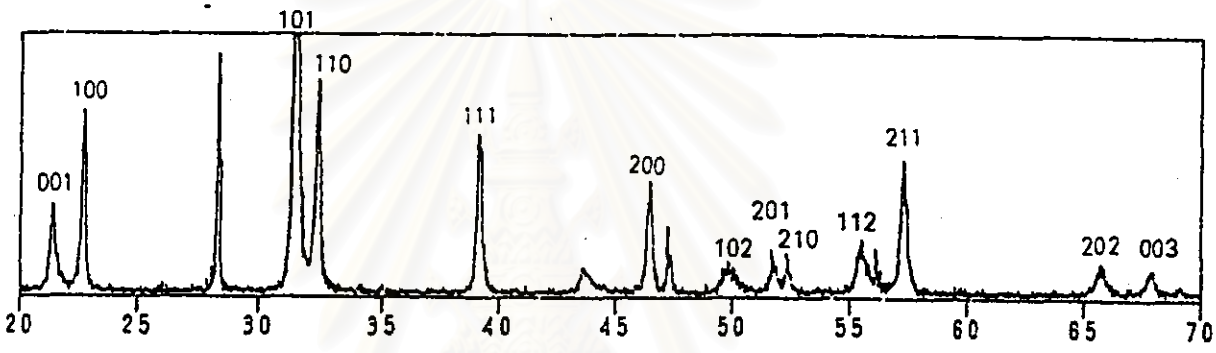

(b)

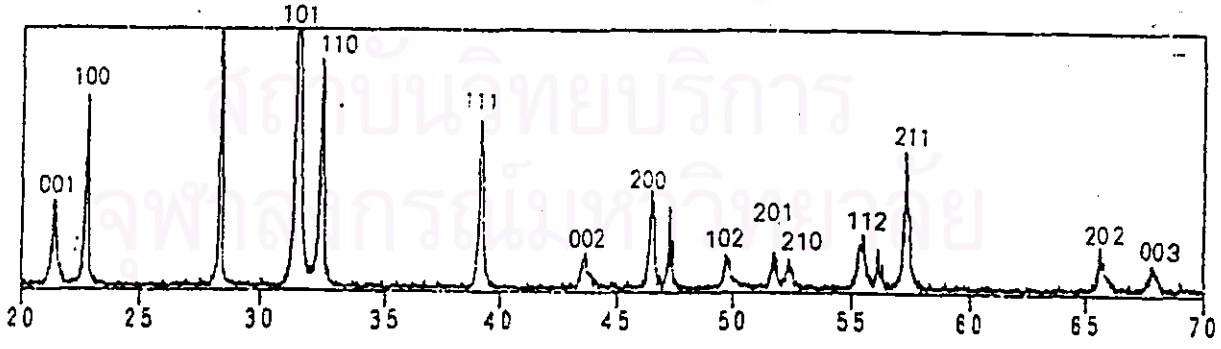

(c)

Fig. 20 The X-ray diffraction patterns of PC5T (50gms) calcined in air at (a) 750°C, (b) 800°C and (c) 850°C for 2 hrs.

4.2 Weight loss and shrinkage

The results of weight loss of all PLT and PCT compositions which were calcined for 2 hrs at 750°C show in table 7 and 8. This may be noted that PLT and PCT compositions showed an increase in weight loss with increasing La^{3+} and Ca^{2+} contents.

The composition with 5%mole La^{3+} content resulted in weight loss of 1.1%. When La concentration was increased up to 20%mole, it gradually increased to 2.1% (see table 7). Similarly, it was observed for PCT samples. When Ca concentration was increased from 5 to 30%mole, the weight loss of samples was in a range of 1.5 to 6.2% (see table 8). In comparison, PCT samples showed a larger weight loss than PLT samples. But undoped-PT composition resulted in larger weight loss than those of PLT and PCT samples. This may imply that Pb volatilization would play a role in calcination. However a higher weight loss in PCT samples obtained may result from the decomposition of CO_2 from $CaCO_3$ as a starting raw material in this study.

Table 9 and 10 showed the results of weight loss and shrinkage of PLT and PCT samples which were sintered for 2 hrs at 1200°C. PLT samples exhibited increasing values of shrinkage and weight loss when La^{3+} concentration of samples was increased. PL5T samples had weight loss and shrinkage of 2.0% and 15.5%, respectively. These weight loss and shrinkage gradually increased up to 3.7 and 16.6% as La^{3+} concentration was raised up to 20%mole (see table 6). For PCT samples, the results of weight loss exhibited decreasing values ranging from 3.5% to 1.3% for PC15T and PC30T, respectively. However, the weight

loss of PC5T and PC10T samples were not observed due to disintegration of the samples during sintering (see table 10). PCT samples showed no significant results of difference in shrinkage. However, PC20T sample had a higher shrinkage value of 16.2% which was no relation of decreasing trend. This reason was not clearly understood. It may note that La^{3+} and Pb^{2+} volatilization resulted in increasing weight loss for PLT samples during sintering and decreasing values of weight loss for PCT samples. This may be due to the decreasing of volatility characteristics.

There was no observation for PT, PC5T and PC10T samples because crack occurred during cooling through the Curie point (T_c). This may be due to highly tetragonality distortion. Similarly, R. Ganesh et al.[31] could not achieve to prepare PCT samples with Ca^{2+} concentration less than 20%mole.

Table 7 %Weight loss of $Pb_{1-x}La_xTi_{1-x/4}O_3$ compositions calcined at 750°C for 2 hrs.

Composition	%Weight loss
PT	5.0
PL5T	1.1
PL10T	1.5
PL15T	1.9
PL20T	2.1

Table 8 %Weight loss of $Pb_{1-x}Ca_xTiO_3$ compositions calcined at 800°C for 2 hrs.

Composition	%Weight loss
PC5T	1.5
PC10T	2.1
PC15T	2.9
PC20T	4.3
PC30T	6.2

Table 9 %Weight loss and % shrinkage of $Pb_{1-x}La_xTi_{1-x/4}O_3$ compositions sintered at 1200°C for 2 hrs.

Composition	%Weight loss	% shrinkage
PT	*	*
PL5T	2.0	15.5
PL10T	3.1	16.4
PL15T	3.6	16.5
PL20T	3.7	16.6

Table 10 %Weight loss and % shrinkage of $Pb_{1-x}Ca_xTiO_3$ compositions sintered at 1200°C for 2 hrs.

Composition	%Weight loss	% shrinkage
PC5T	*	*
PC10T	*	*
PC15T	3.5	15.3
PC20T	2.2	16.2
PC30T	1.3	15.2

Remark : * PT , PC5T , and PC10T were not prepared .

4.3 Microstructure analysis

Microstructure characterization of the fractured cross-section of PLT and PCT samples sintered at 1200°C for 2 hrs was determined.

The structure of PLT samples shows in fig. 21 and 22. Results of PL5T, PL10T, PL15T, and PL20T samples exhibited grain sizes in the range of 0.2 - 1.0 μm, 0.5 - 2 μm, 1 - 3 μm, and 1-5 μm, respectively. Grain size of PLT system increased with increasing La^{3+} concentration. From micrographs of all samples, there are no significant differences in amounts of pores present and pore sizes. Pore sizes are in the range of 0.5 - 5 μm. It may note that pore sizes are not dependent on the amount of La^{3+} dopant.

From the results of SEM photomicrographs, the small seeds can be observed around the grain boundaries for the compositions of PL15T and PL20T as the arrows marked in fig.21. When these seeds (< 1 μm) were examined by EDS (Energy Dispersive Spectroscopy) , a different phase could not be identified. This may be attributed to the limitation of EDS resolution.

For PCT compositions , the microstructures show that the grain sizes decrease with increasing Ca^{2+} contents as shown in fig.23 and 24. For PC15T compositions, the grain sizes are in the range of 50-100 μm. and cracks were observed along the grain boundaries. Pores were found inside grains and grain boundaries. Compositions of PC20T exhibited microstructure similar to PC15T samples. However, the grain sizes varied from 5-100 μm. Cracks along grain boundaries appeared less than those of PC15T samples and the grain growth was

likely observed. When PC30T samples were examined the microstructure was denser. Cracks were not significant and grain sizes decreased to a range of 2-20 μm. These results imply that Ca^{2+} substitution for Pb^{2+} ions may result in inhibiting grain growth.

In general, the grain sizes of PCT samples are greater than that of PLT samples. Since the atomic size of Calcium ions is smaller than Lanthanum ion therefore substitution of Ca^{2+} ions for Pb^{2+} ion would lead to the highly tetragonality distortion.

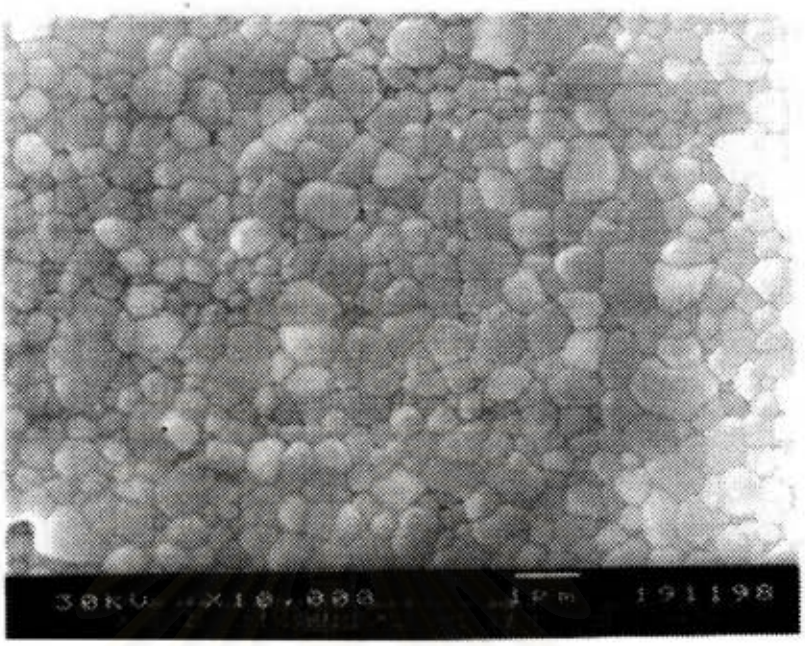

(a)

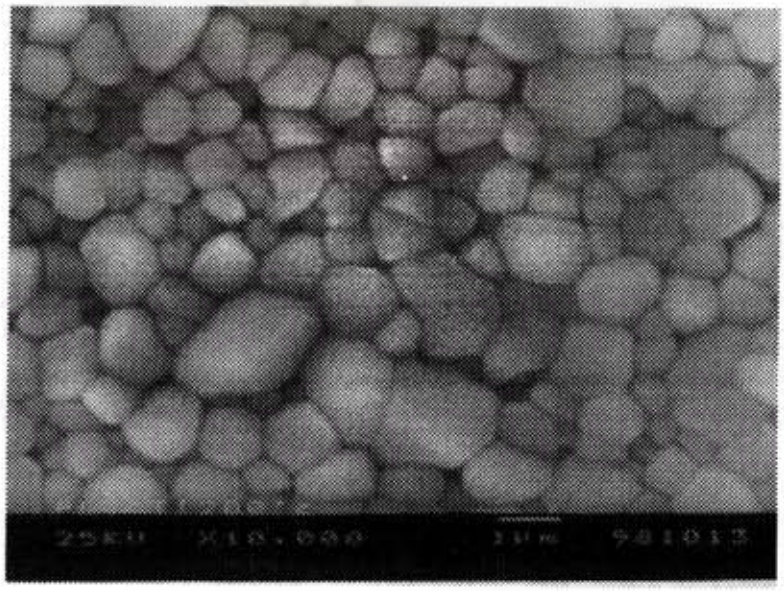

(b)

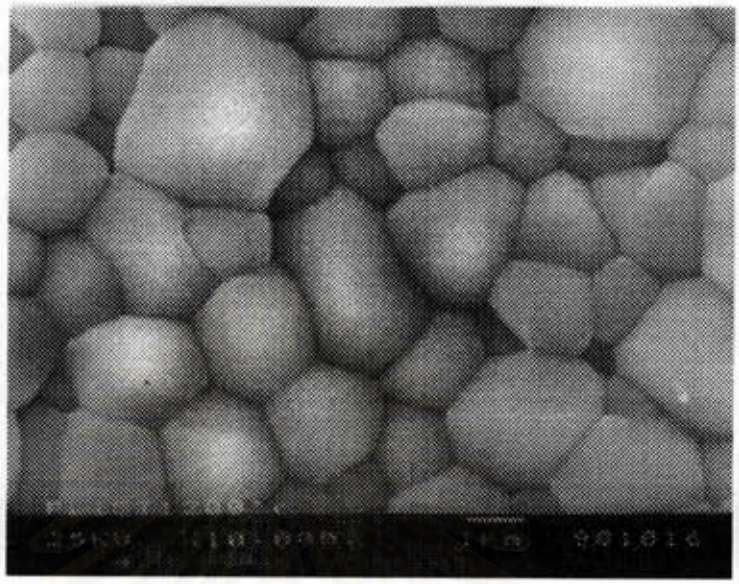

(c)

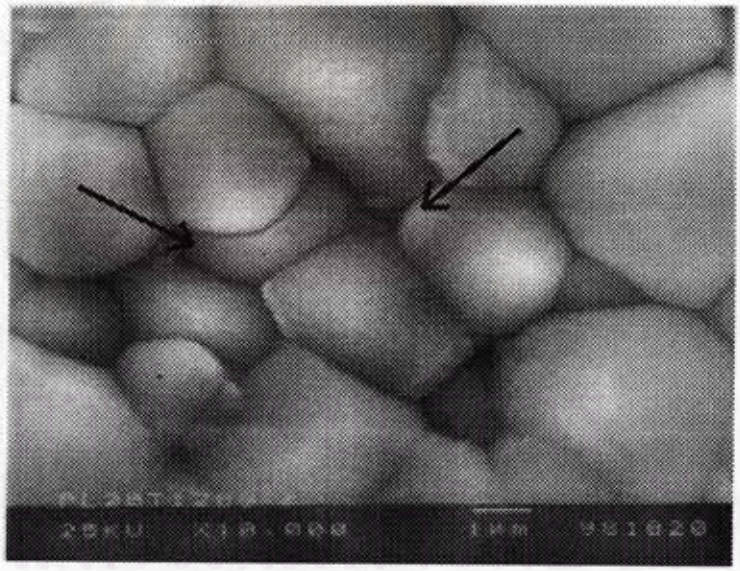

(d)

Fig. 21 SEM micrographs of the PLT compositions sintered at 1200°C for 2 hrs: (a) PL5T ; (b) PL10T ; (c) PL15T and (d) PL20T at (× 10,000)

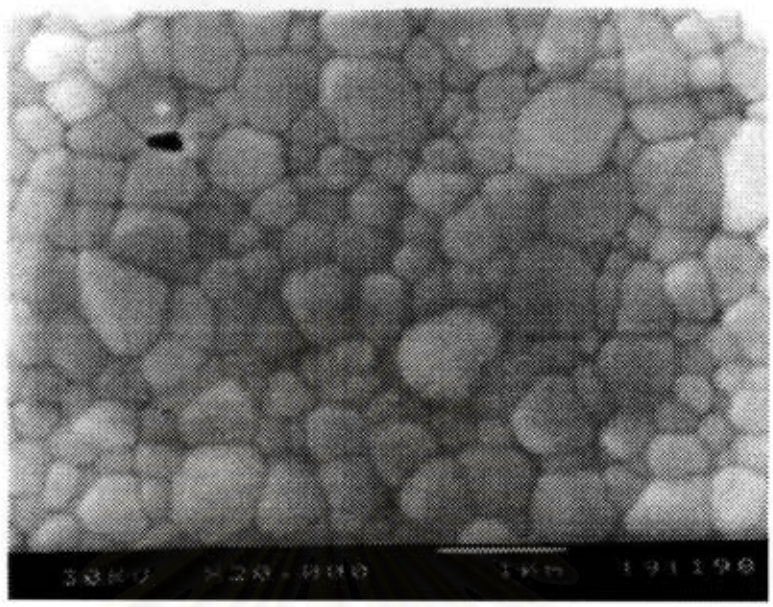

(a)

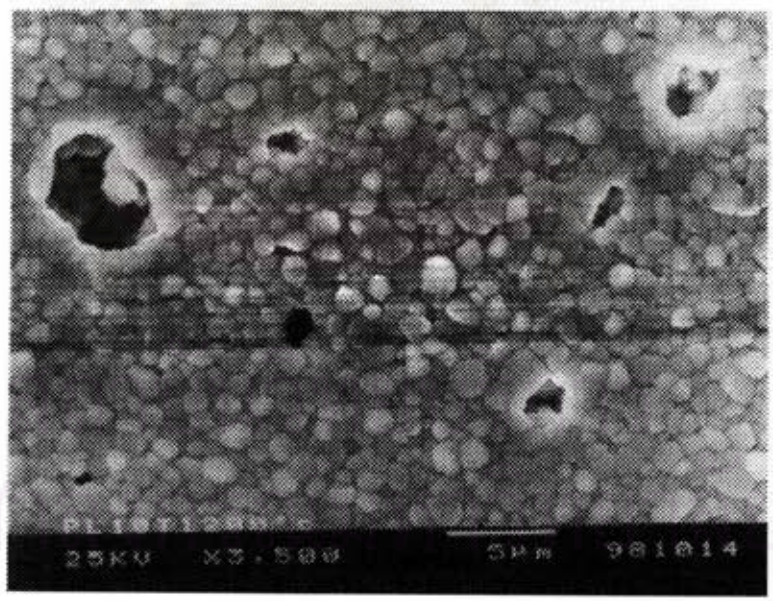

(b)

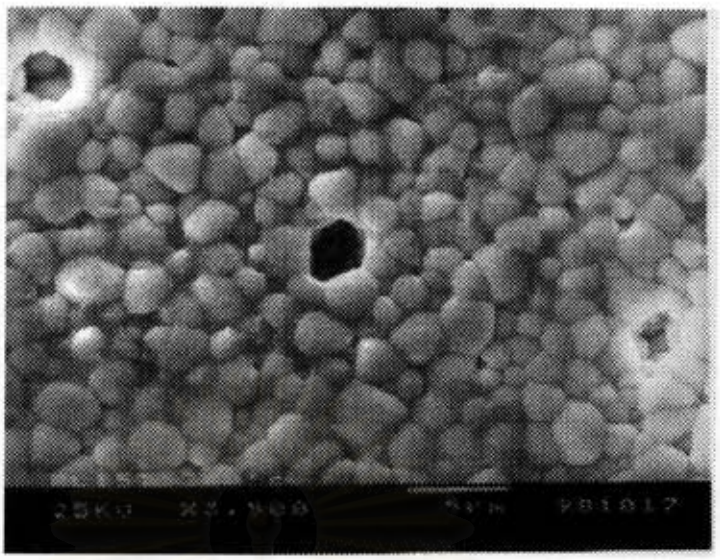

(c)

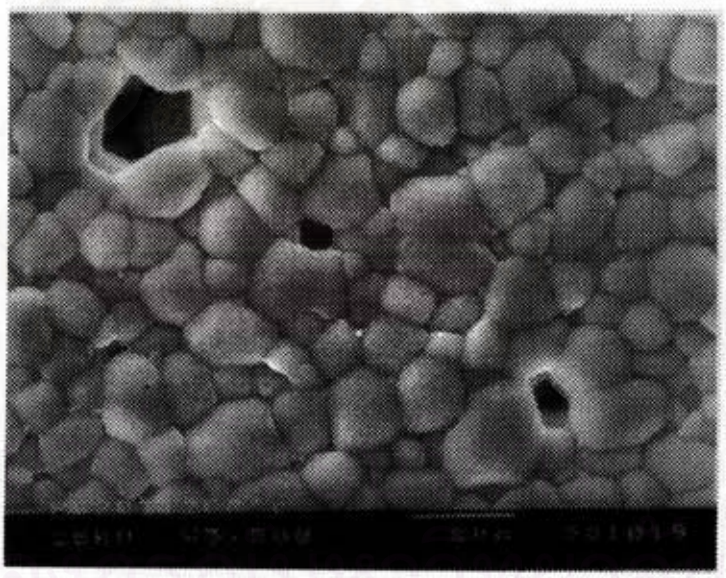

(d)

Fig. 22 SEM micrographs of PLT compositions sintered at 1200°C for 2 hrs (a) PL5T (×20,000) ; (b) PL10T (×3,500) ; (c) PL15T (×3,500) and (d) PL20T (×3,500).

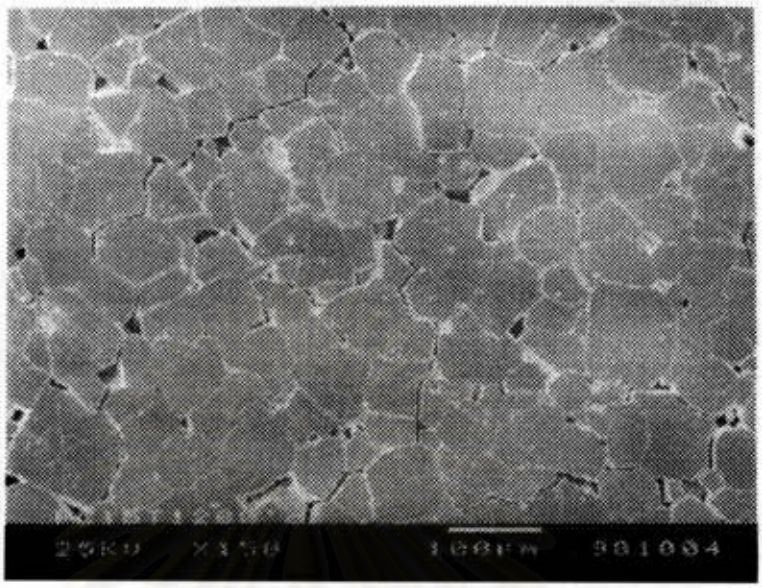

(a)

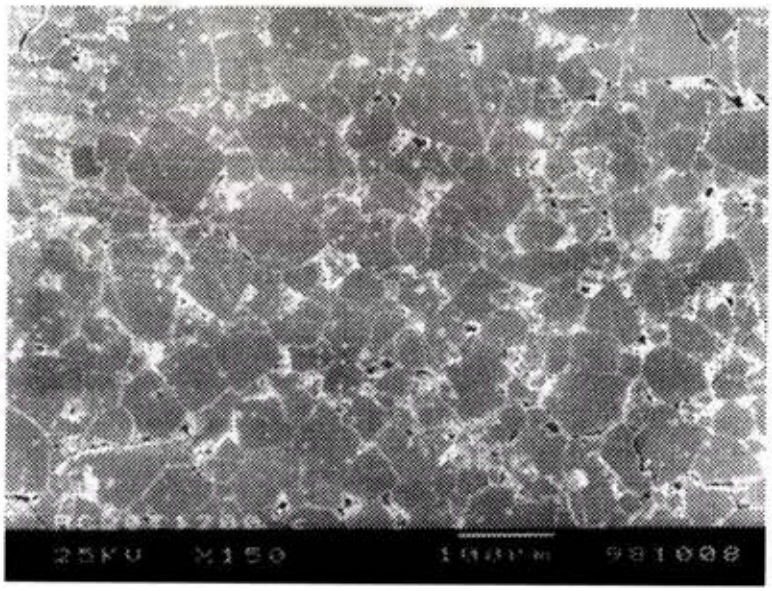

(b)

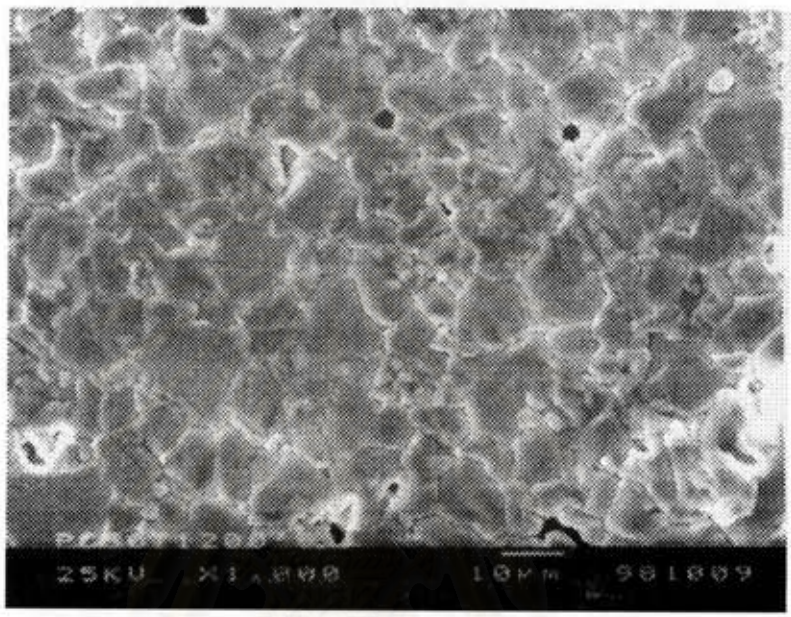

(c)

Fig.23 SEM micrographs of PCT compositions sintered at 1200°C for 2 hr : (a) PC15T (×150); (b) PC20T (×150) and (c) PC30T (×1,000)

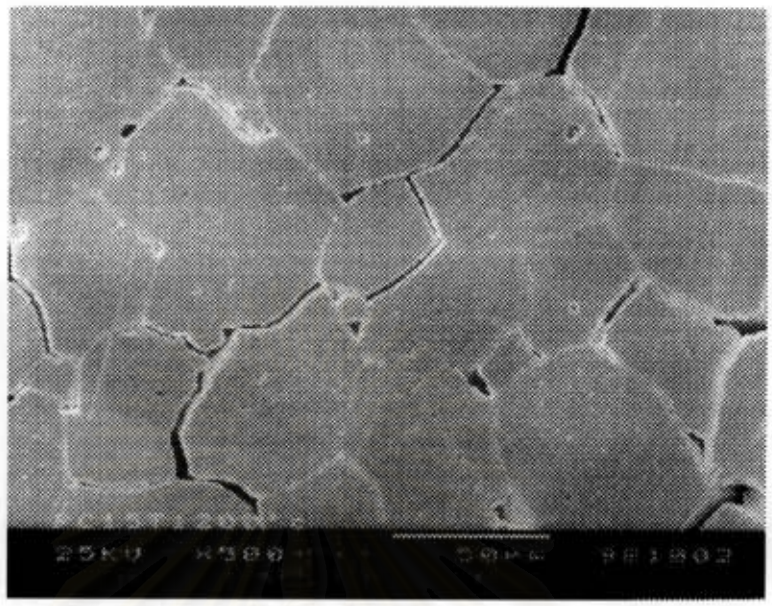

(a)

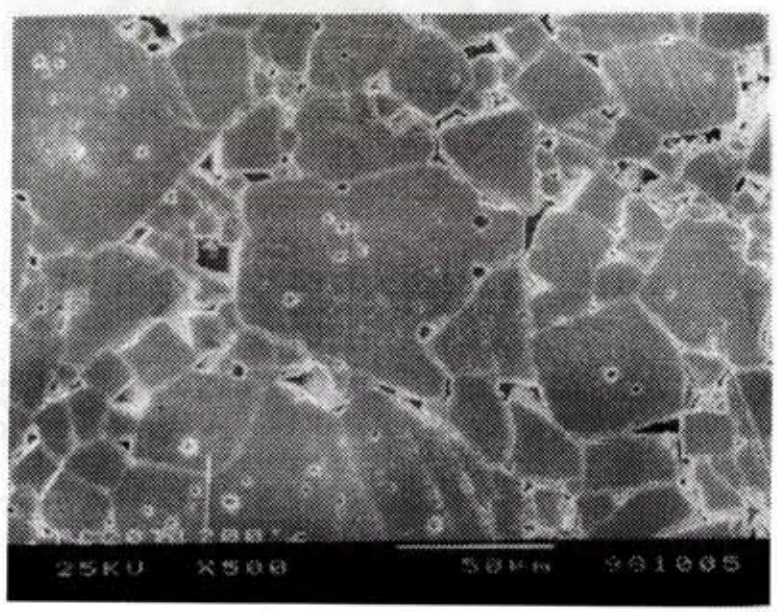

(b)

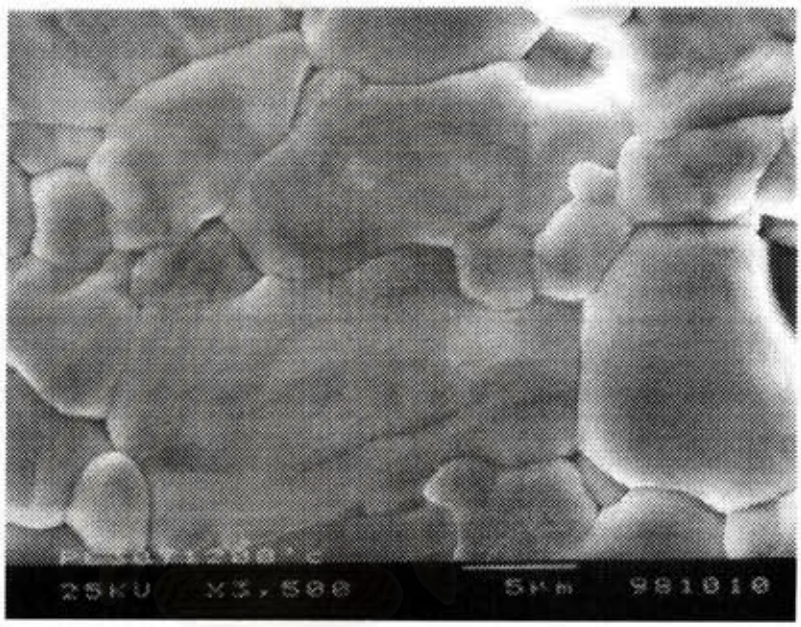

(c)

Fig. 24 SEM micrographs of PCT compositions sintered at 1200°C for 2 hrs (a) PC15T (×500) ; (b) PC20T(×500) and (c) PC30T at (×3,500)

4.4 X-ray diffraction analysis

The X-ray diffraction (XRD) patterns of PLT compositions calcined at 750°C for 2 hrs using a heating rate of 2°C/min and a cooling rate of 5°C/min are shown in fig.25. The results indicate that all compositions have the tetragonal perovskite structure. The XRD pattern of PL5T composition shows a single phase. However, other phases were detected in the compositions with higher La^{3+} content from 10%mole since two peaks appeared at 2θ around 27° and 31°. They were assumed to be unreacted of TiO_2 and PbO raw materials as shown in fig 21. The DTA traces of PL20T before and after calcination can be observed in fig.27. These results show that the reactions should be complete at 750°C since there are no reaction peaks appeared above this temperature. However, the DTA result of PL20T powder calcined at 750°C does exhibit an exothermic peak around 300°C. This may be due to a large amount of powder (50 gms) employed during calcining. Hold for 2 hrs at 750°C is not enough for this amount of powder. A longer soaking time is required to complete the reactions. This also applies to the compositions of PL10T , PL15T and PL20T. However, the XRD patterns of PL20T pellet sintered at 1200°C for 2 hours with a heating rate of 4°C/min and cooling rate of 5°C/min. exhibited a single phase and complete reaction was obtained (see fig. 28).

The corresponding c and a lattice parameters of PCT and PLT with various compositions were determined and results exhibited the c/a values in table 11 and 12. The c/a ratio of calcined samples were higher than those of sintered samples ; These similar results was observed by P.L. Tan et al.[47] . It can be noted that the c/a ratio for sintered samples should give more accurate

value than that of which calcined sample. This may be attributed to that a homogeneous solid solution was obtained during sintering.

Fig. 29 and 30 show the lattice parameters and c/a ratio of calcined powder and sintered ceramic. The a-lattice parameter of both calcined powder and sintered ceramics showed a slight increase with increasing La^{3+} content , ranging from 3.904 A° for calcined PL5T to 3.913 A° for calcined PL20T and from 3.903 A° for sintered PL5T to 3.941 A° for sintered PL20T. The c-lattice parameter decreased more noticeably with increasing La^{3+} content. For example, the c axis for PL5T calcined powder equals 4.129 A° reducing to 4.081 A° for PLT with 20%mole La^{3+} whilst the c axis for PL5T bulk ceramics equal 4.066 A° reducing to 4.000 A°. The changing in lattice parameter with increasing concentration may imply that substitution of La^{3+} ion for Pb^{2+} ions in the $PbTiO_3$ unit cell lattice was produced.

Compositions of PCT were obtained from calcination in air at 800°C for 2 hours using a heating rate of 2°C/min and cooling rate of 5°C/min. Their X-ray diffraction patterns are shown in fig.31. The XRD pattern of PC5T samples showed a single phase tetragonal structure. When the Ca^{2+} level was increased up to 15 %mole , the small peak at 2θ ~33° was detected. When Ca^{2+} content was increased up to 30 %mole , this peak was significant and it was corresponded to the XRD pattern of $CaTiO_3$ as shown in fig 32. Fig.33 shows the X-ray patterns without a peak at 2θ ~33°of PC30T sample sintered at 1200°C for 2 hours and a single phase was clearly obtained. It may be suggested that samples with a homogeneous solid solution were obtained at the sintering temperature.

From the X-ray diffraction data, the lattice parameters and their tetragonality (c/a ratio) as a function of Ca^{2+} content for calcined powder are shown in fig. 29. The a-lattice slightly increased with increasing Ca^{2+} level and the c/a ratio decreased on approaching the tetragonal-to-cubic phase boundary. These results indicated that the crystal tetragonality changed. Table 9 shows the variation in the c/a ratio as a function of Ca^{2+} content in sintered specimens. The c/a ratio for PC15T and PC30T samples were calculated to be a range of ~ 1.03. But that of PC20T (c/a = 1.050) was higher. These results showed no corresponding trends for PCT calcined powders. This may be attributed to PbO volatilization.

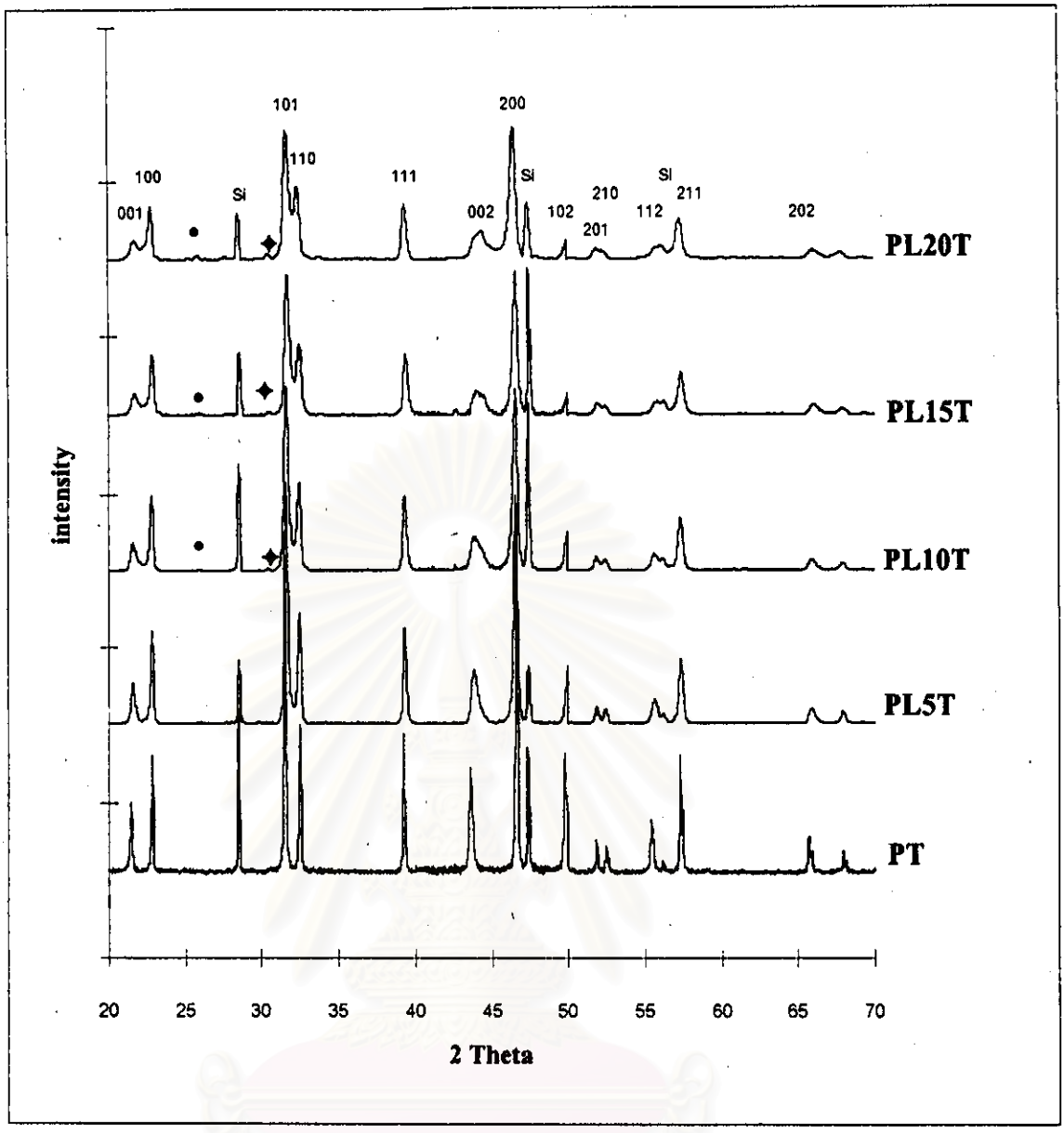

Fig. 25 X-ray diffraction patterns of $Pb_{1-x}La_xTi_{1-x/4}O_3$ (x = 0.05 , 0.10 , 0.15 , 0.20) powder calcined at 750°C for 2 hrs

- TiO_2
- ✦ PbO

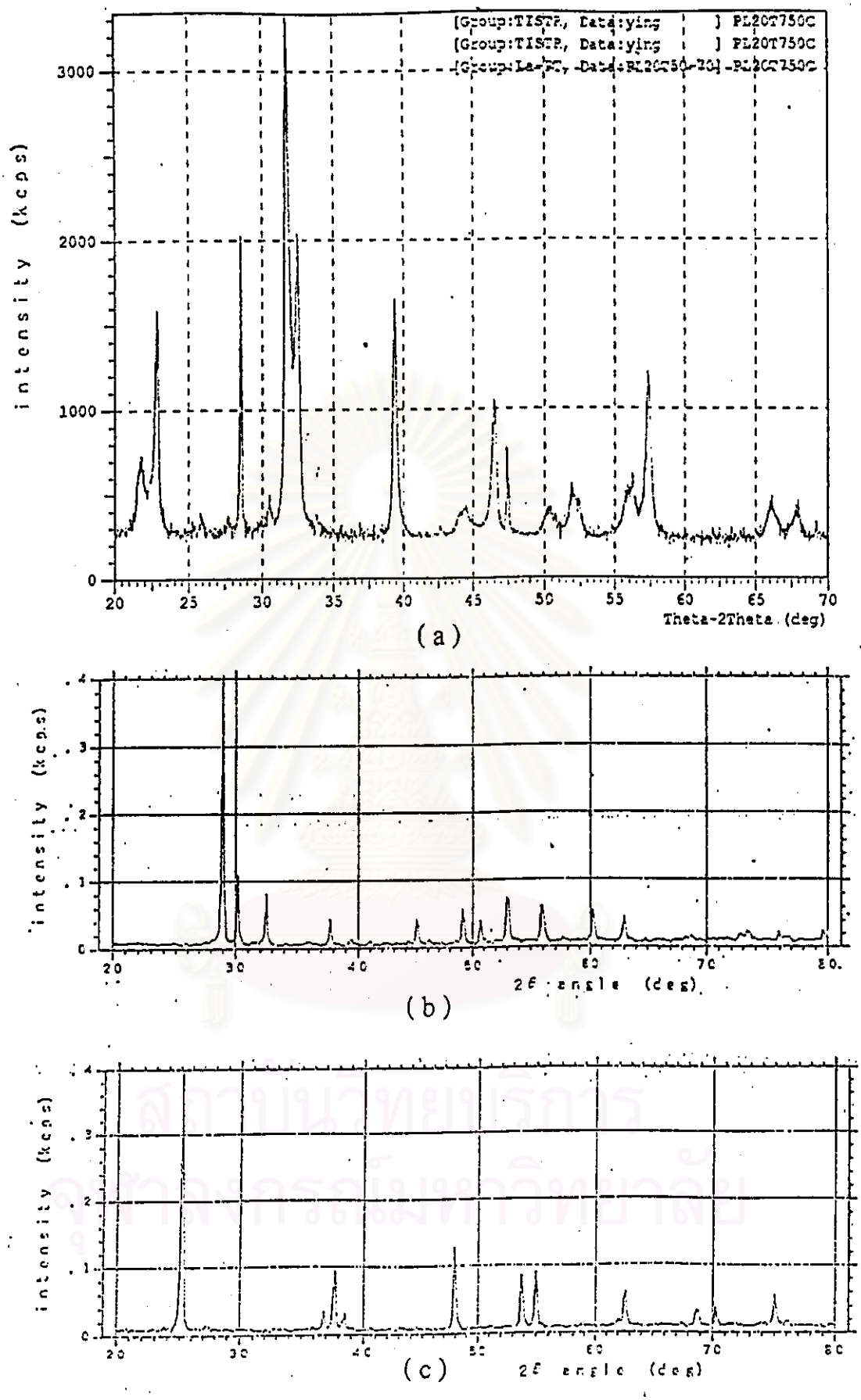

Fig. 26 X-ray diffraction patterns ; (a) PL20T, (b) PbO, (c) TiO_2

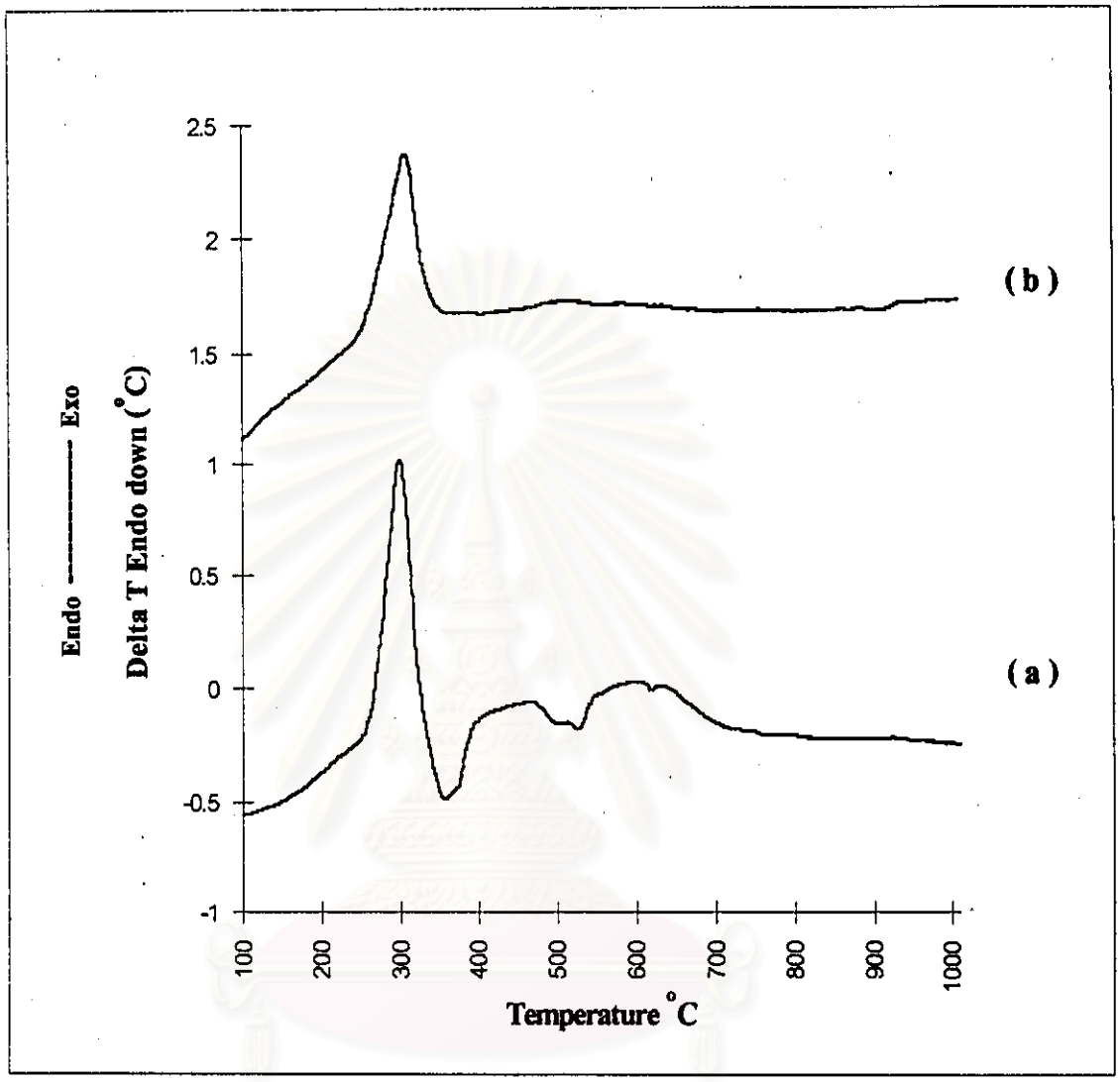

Fig. 27 DTA traces of PL20T powder ; (a) before calcination (b) after calcination at 750°C for 2 hrs using a heating rate of 2°C/min.

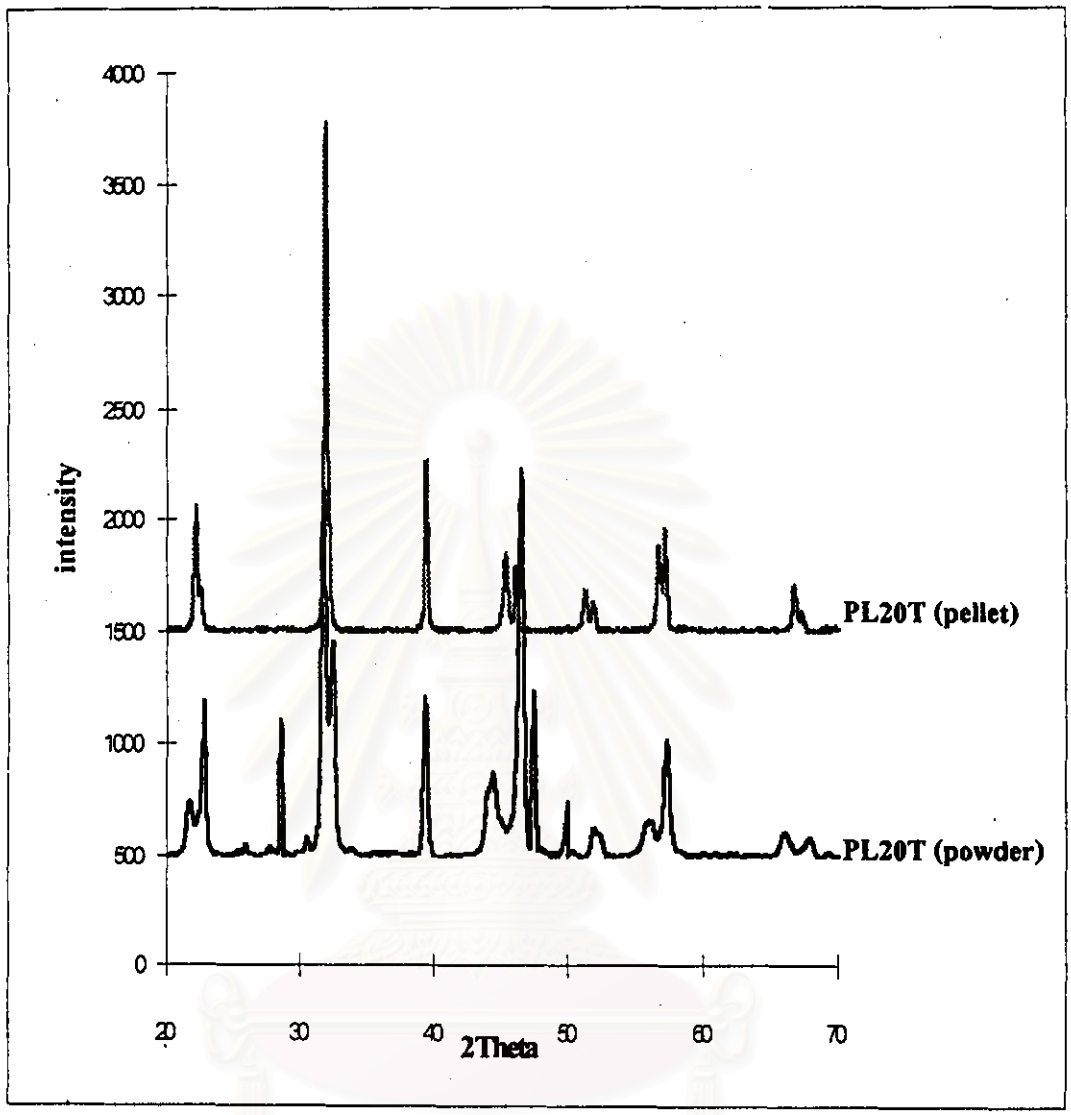

Fig 28 X-ray diffraction patterns of PL20T powder calcined at 750°C for 2 hrs and PL20T pellet sintered at 1200°C for 2 hrs

Table 11 The c/a values of PLT calcined powder and sintered ceramics

sample	calcined powder	sintered ceramic
PT	1.064	*
PL5T	1.058	1.042
PL10T	1.056	1.033
PL15T	1.053	1.023
PL20T	1.043	1.015

Table 12 The c/a values of PCT calcined powder and sintered ceramics

sample	calcined powder	sintered ceramic
PT	1.064	*
PC5T	1.063	*
PC10T	1.056	*
PC15T	1.053	1.038
PC20T	1.051	1.050
PC30T	1.048	1.036

For sintered ceramic, the Si standard was used to the external reference.

Remark : * PT, PC5T and PC10T could not be prepared in a dense form

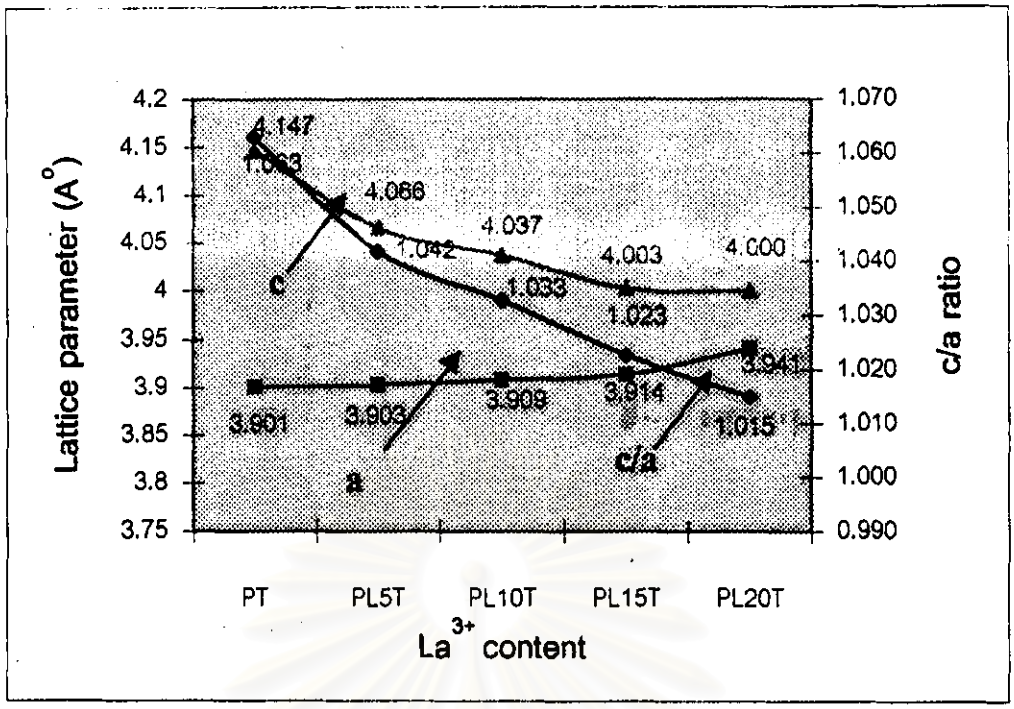

Fig. 29 Lattice parameter and c/a ratio for sintered specimens of PLT compositions

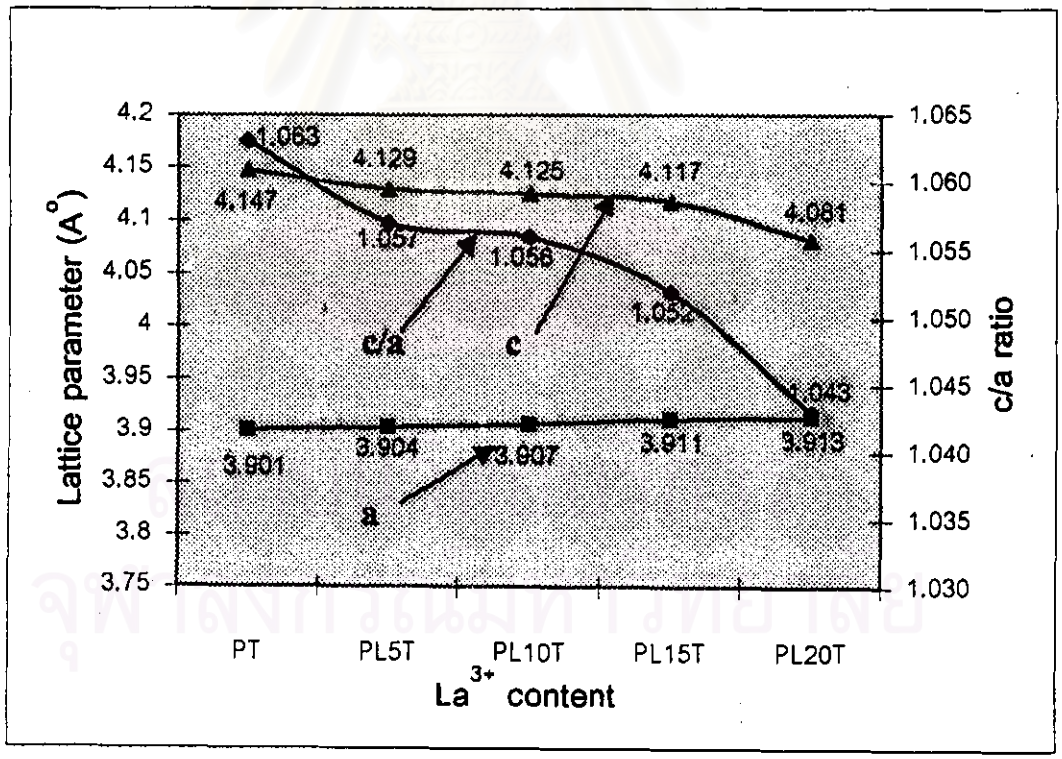

Fig. 30 Lattice parameter and c/a ratio for calcined powder of PLT compositions

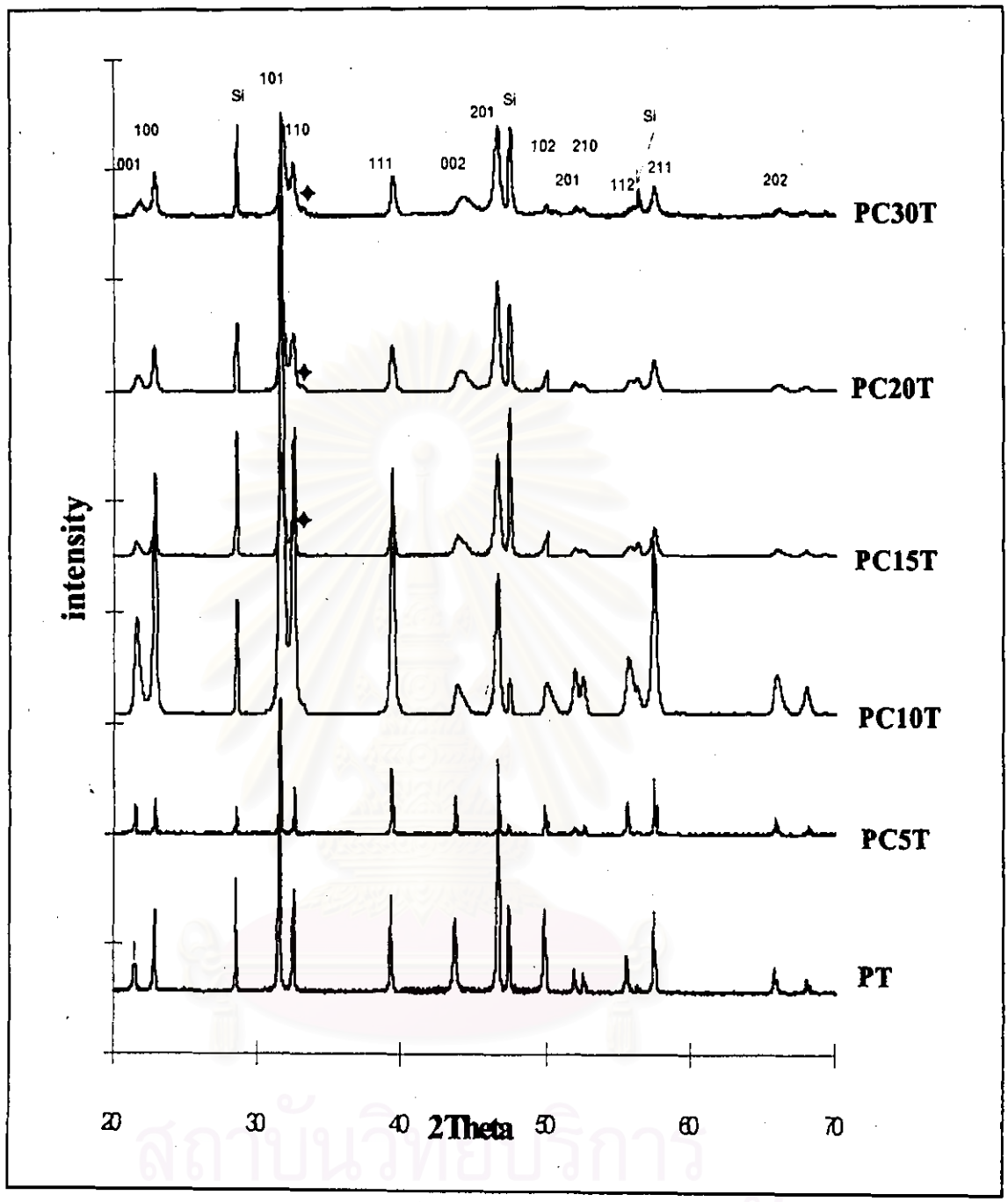

Fig 31 X-ray diffraction patterns of $Pb_{1-x}Ca_xTiO_3$ (x = 0.05 , 0.10 , 0.15 , 0.20 and 0.30) powder calcined at 800°C for 2 hrs

✦ $CaTiO_3$

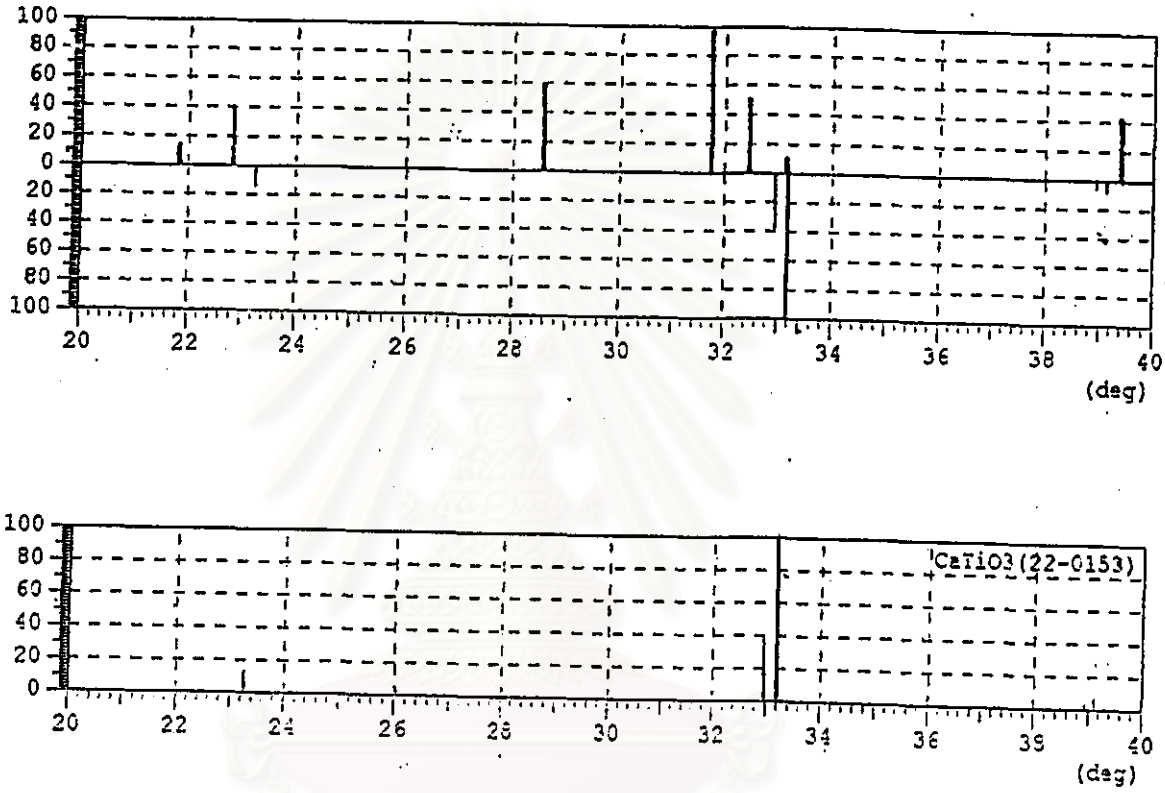

Fig 32 X-ray diffraction patterns of PC30T and $CaTiO_3$

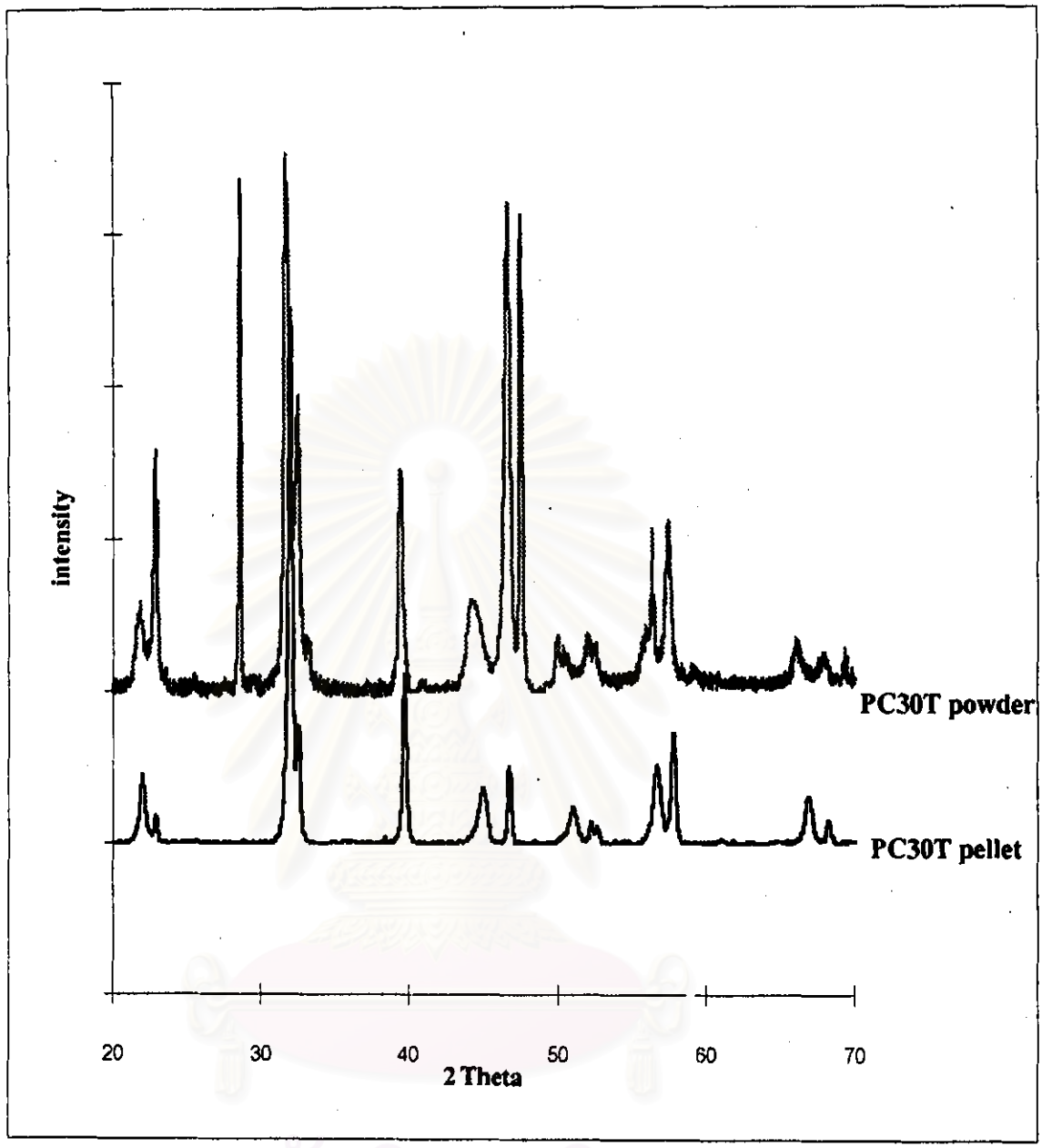

Fig 33 X-ray diffraction patterns of PC30T powder calcined at 800°C for 2 hrs and PC30T pellet sintered at 1200°C for 2 hrs

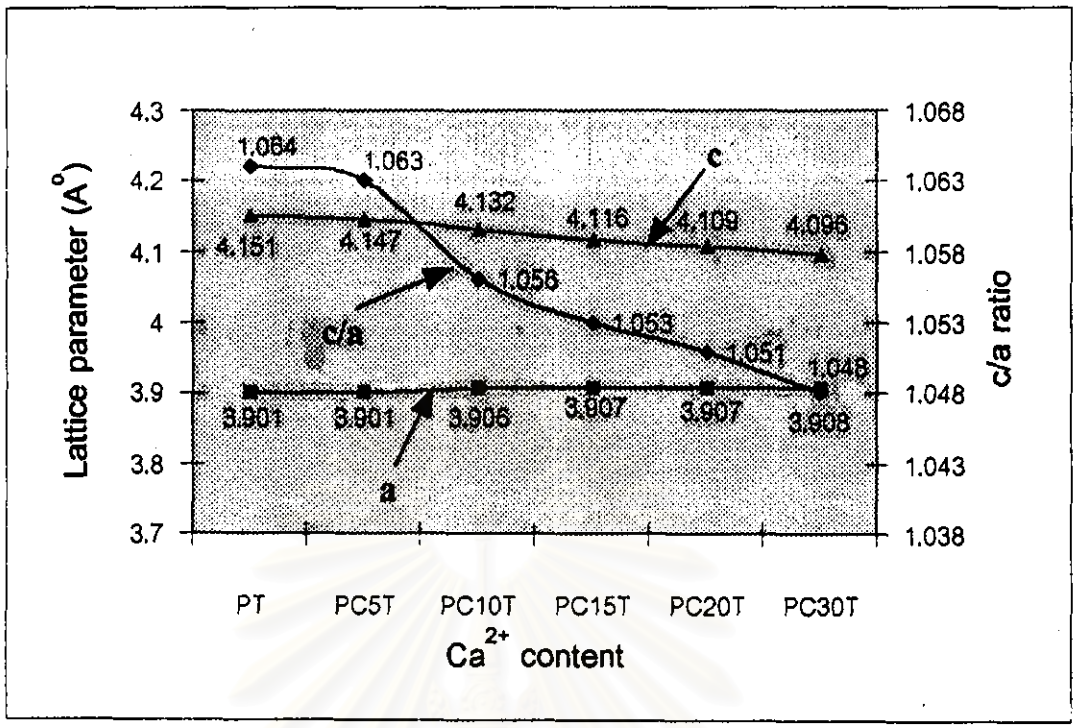

Fig. 28 Lattice parameter and c/a ratio for calcined powder of PCT compositions

Electrical Properties

Electrical measurements were carried out for $Pb_{1-x}La_xTi_{1-x/4}O_3$ ($0.05 \leq x \leq 0.20$) and $Pb_{1-x}Ca_xTiO_3$ ($0.15 \leq x \leq 0.30$) specimens. The electrical properties of PT, PC5T and PC10T were not investigated due to the cracking problem. The electroded specimens were characterized to investigate the electrical properties such as dielectric constant (K') , dielectric loss (D) and polarization vs electric field (hysteresis loop) at room temperature and the Curie temperature (T_c) for the PL15T and PC15T compositions.

4.5 The dielectric constant (K') and dielectric loss (D) at room temperature

The dielectric constant (K') and dielectric loss (D) as a function of La^{3+} concentration at 1 kHz are exhibited in fig. 35. The dielectric constant (K') increases with increasing La^{3+} content, for example the dielectric constant of PL5T is about 412 and about 603 for PL15T. When PLT contained 20%mole La^{3+}, its dielectric value significantly increased up to ~ 1281. PLT composition with 5 - 15%mole La^{3+} and dielectric loss (D) were quite stable ranging from 0.05 to 0.06. Whilst, the PL20T composition resulted a high dielectric loss (D = 0.58).

The dielectric constant (K') and dielectric loss (D) as a function of the frequency (1, 10, 100 kHz) of PLT compositions were examined, fig. 36-39. PLT compositions with La^{3+} content ranging from 10-20%mole resulted decrease in dielectric constant values with increasing frequencies. But PL20T samples

exhibited increasing dielectric constant value when frequency levels were raised, fig 39.

For study of dielectric loss as a function of frequency, PL5T samples exhibited no significant difference in dielectric loss as various frequencies were applied for measurement. The trend of decreasing in dielectric loss at higher was observed for PL10T and PL20T samples. For PL15T samples as shown in fig. 38, a high dielectric loss was detected at a high frequency. Results of dielectric loss had no similar trend; this may be attributed to sample defects during preparation. However, the reason was not clearly understood.

For PCT system, fig. 40 displayed the values of dielectric constant (K') and dielectric loss (D) as a function of Ca^{2+} concentration at a frequency of 1 kHz. The dielectric constant (K') showed decreasing values with Ca^{2+} concentration ranging from 15 to 20%mole but PC30T composition had dielectric constant of 192 which was higher than that of PL20T composition. Pores and cracks of PC20T in microstructure analysis may indicate a part problem of the very low dielectric constant. However, the reason for these results was not clearly understood. The dielectric loss (D) decreased with increasing Ca^{2+} concentration; an example of dielectric loss of 1.207 for PC15T gradually reduced to 0.066 for PC30T composition.

When the dielectric constant (K') and dielectric loss (D) as a function of the frequency (1, 10, 100 kHz) of PCT compositions are examined. Fig. 41-43 showed dielectric constant and dielectric loss of all PCT compositions, those electrical property values decreased with increasing the frequencies.

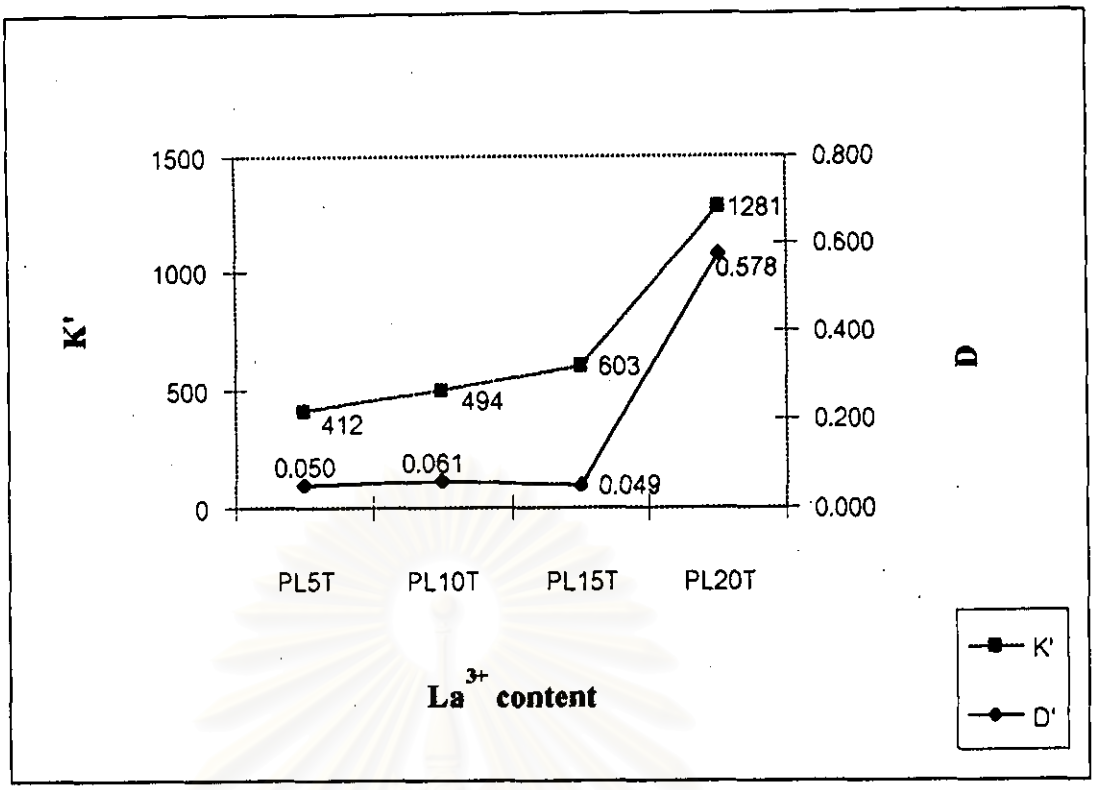

Fig.35 The dielectric constant (K′) and dielectric loss (D) as a function of La^{3+} content of $Pb_{1-x}La_xTi_{1-x/4}O_3$ at a frequency of 1 kHz.

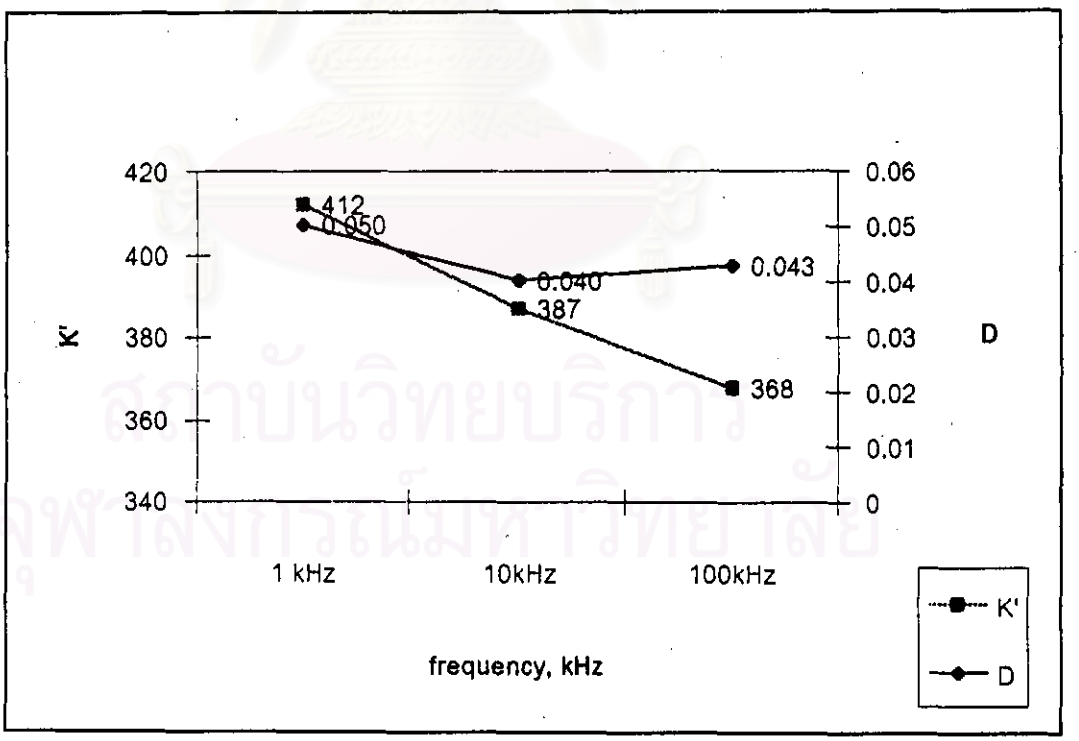

Fig 36 Dielectric constant (K′) and dielectric loss (D) vs frequencies of PL5T composition sintered at 1200°C for 2 hrs

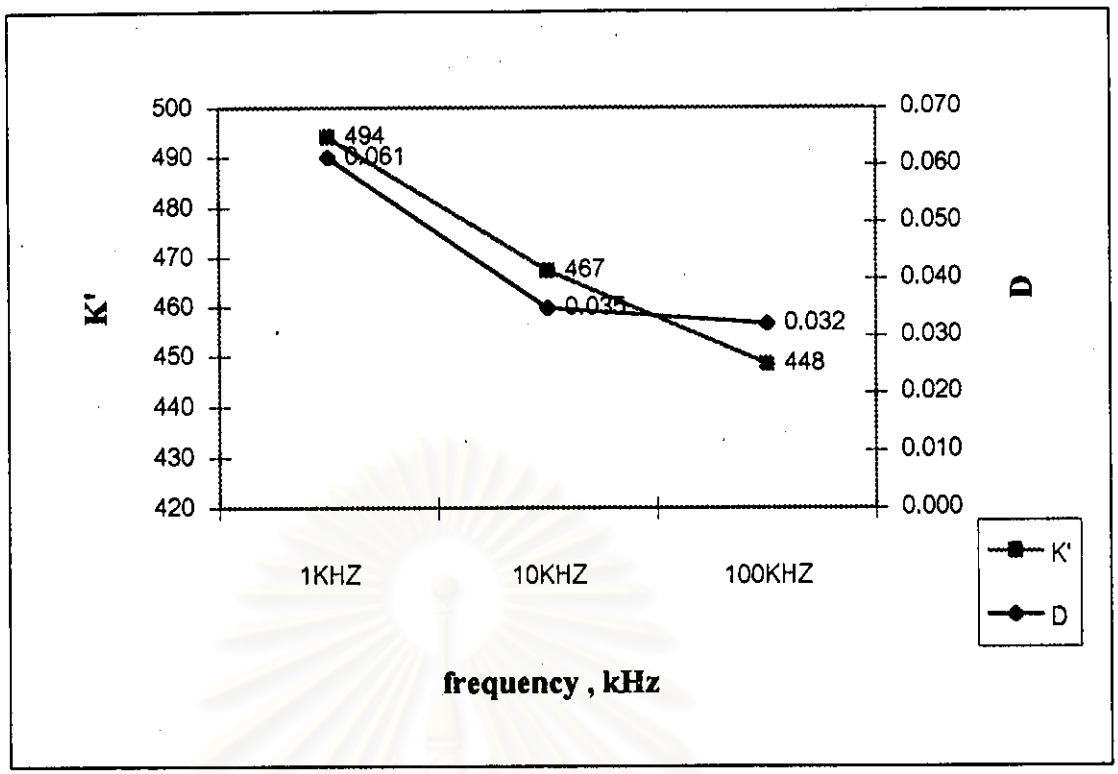

Fig 37 Dielectric constant (K') and dielectric loss (D) vs frequencies of PL10T composition sintered at 1200°C for 2 hrs

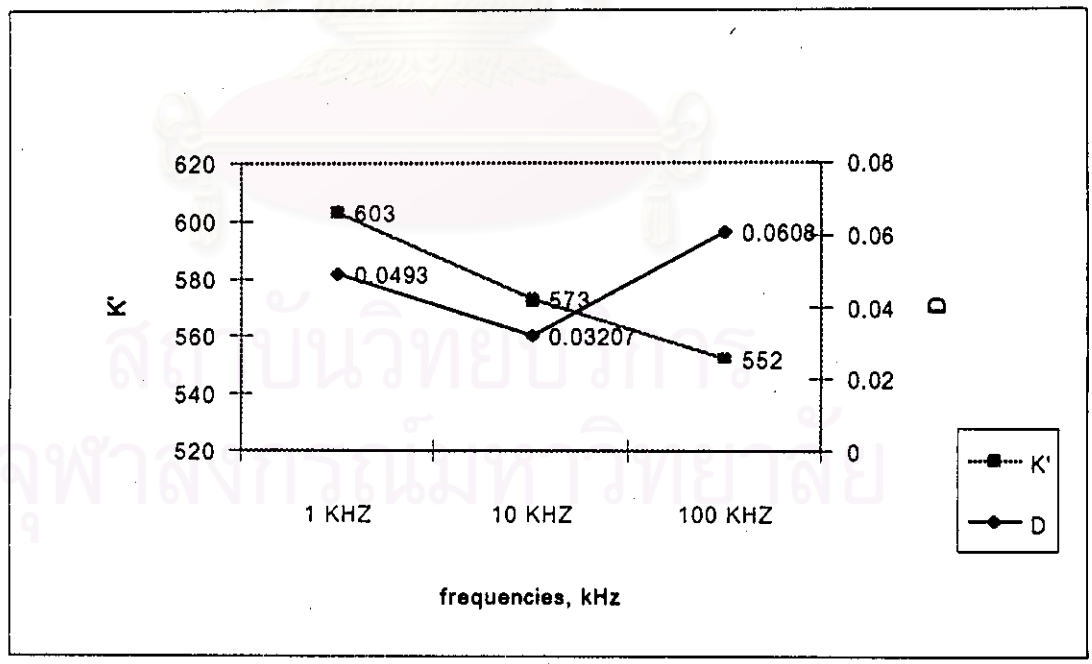

Fig. 38 Dielectric constant (K') and dielectric loss (D) vs frequencies of PL15T composition sintered at 1200°C for 2 hrs

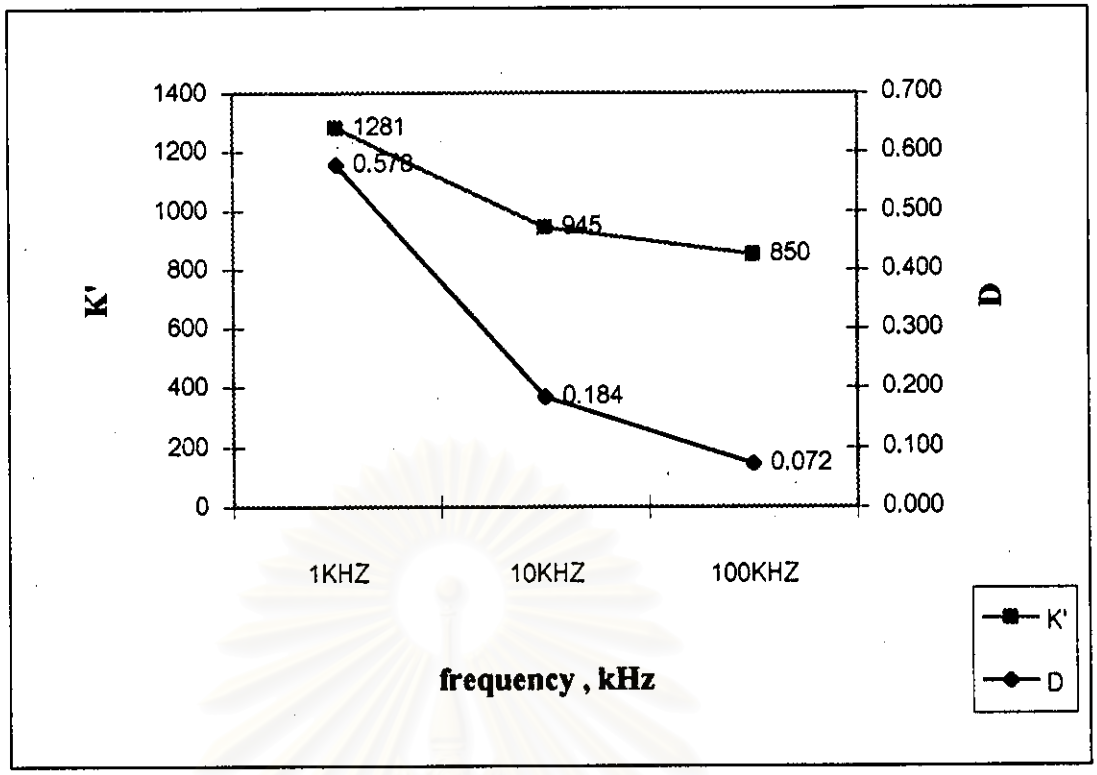

Fig 39 Dielectric constant (K') and dielectric loss (D) vs frequencies of PL20T composition sintered at 1200°C for 2 hrs

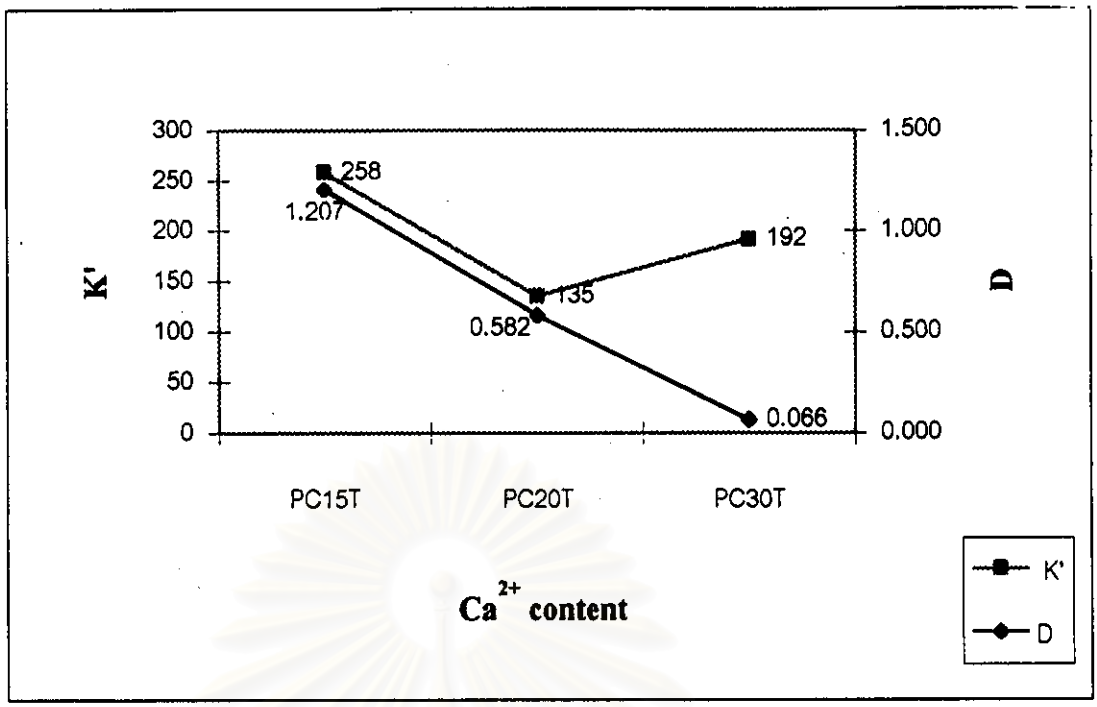

Fig.40 The dielectric constant (K') and dielectric loss (D) as a function of Ca^{2+} content of $Pb_{1-x}Ca_xTiO_3$ measured at 1 kHz.

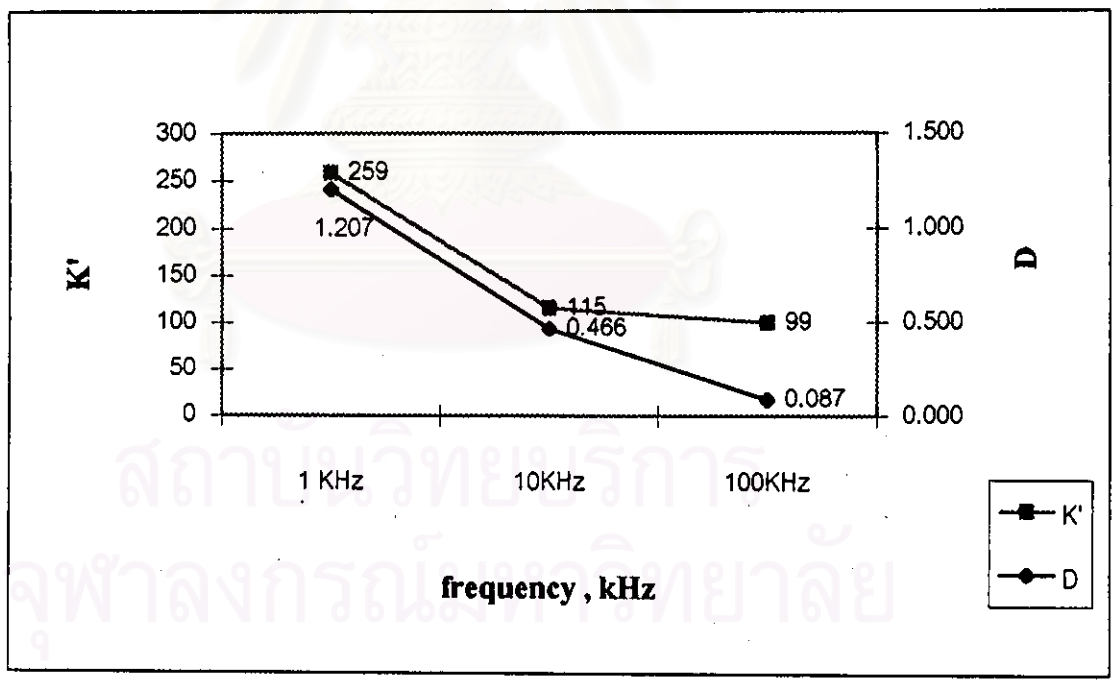

Fig.41 The dielectric constant (K') and dielectric loss (D) vs frequencies of PC15T composition sintered at 1200°C for 2 hrs

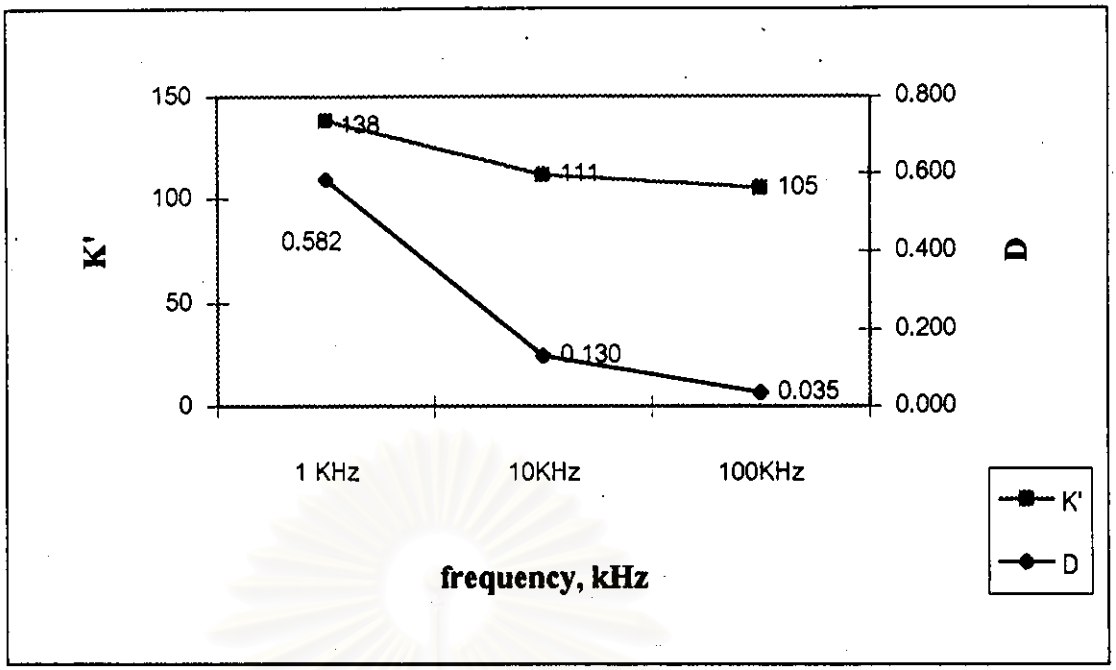

Fig 42 Dielectric constant (K') and dielectric loss (D) vs frequencies of PC20T composition sintered at 1200°C for 2 hrs

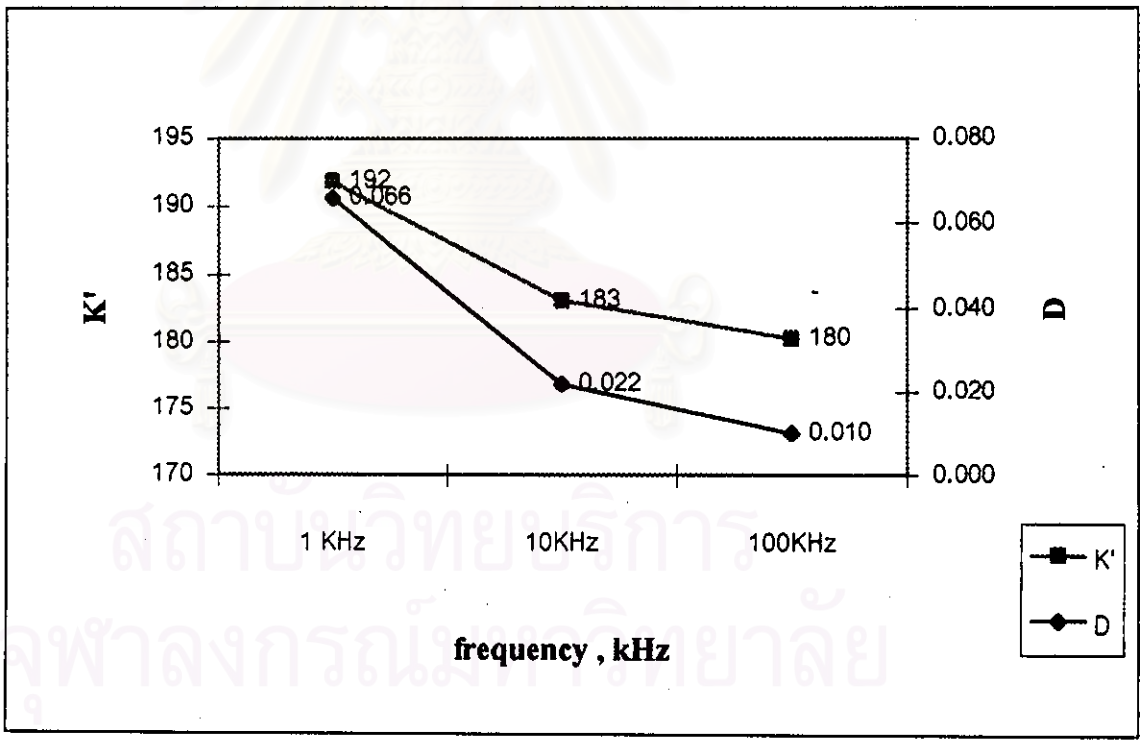

Fig. 43 Dielectric constant (K') and dielectric loss (D) vs frequencies of PC30T composition sintered at 1200°C for 2 hrs

4.6 The dielectric constant (K') and dielectric loss (D) as a function of temperature at the frequencies of 10, 100 kHz and 1 MHz

The dielectric constant (K') and dielectric loss (D) of PL15T composition as a function of temperature are determined in fig. 44 and 45, respectively. It is generally observed that the dielectric constant increased sharply approaching at the Curie point like those of $BaTiO_3$. In similar manner of observation, the Curie point value of PL15T composition was estimated about 255°C when a dielectric value was 10189 at 10 kHz. When the frequencies were raised from 100 to 1000 kHz, the maximum dielectric constants increased from 10023 to 11212 (see table 13). For T_c and K' measurement at 10 kHz the results studies were large values observed by T. Yamamoto[42] ($T_c \sim 245$°C and $K' \sim 9700$).

For the dielectric loss (D) measurement, PL15T samples exhibit phase transformation of ferroelectric to paraelectric. Maximum dielectric loss values at different temperatures; for example, when a measurement frequency was 1 MHz, a maximum (D) was observed at ~ 190°C and a dielectric loss reading was recorded as 0.05. The maximum dielectric loss in a ferroelectric region was found at 230°C and 225°C for frequencies of 10 kHz and 100 kHz, respectively. However, at 255°C, as the Curie temperature, the dielectric loss of all frequencies studied was minimum.

The dielectric constant (K') of PC15T composition as a function of temperature was investigated. Fig. 46 showed a broaden peak of dielectric constant than those of PL15T. The Curie point value was estimated about 280°C

with a dielectric constant of 5229. At higher frequencies of 100 and 1000 kHz, the maximum dielectric constant values decreased (see table 14). The dielectric constant of 5229 at T_c~280°C is similar to R. Ganesh 's report [36].

Dielectric loss showed a maximum value of 0.5 at a temperature of 250°C. But these maximum dielectric loss values were detectable for frequencies of 100 kHz and 1 MHz. However, as the dielectric constant reached the highest value, dielectric loss was likely minimized.

In general, a dielectric constant value reaches a maximum value and gradually decreases at higher temperature. This appearance was attributed to phase transition from ferroelectric to paraelectric. The Curie point can be read out, as well as dielectric constant values of approaching phase transformation.

Table 13 The maximum dielectric constant (K') and Curie temperature of PL15T as a function of frequency.

Frequency (kHz)	Maximum K'	Curie point °C (Tc)
10	10189	255
100	10023	255
1000	11212	255

Table 14 The maximum dielectric constant (K') and Curie temperature of PC15T as a function of frequency.

Frequency (kHz)	Maximum K'	Curie point °C (Tc)
10	5229	280
100	4758	280
1000	4846	280

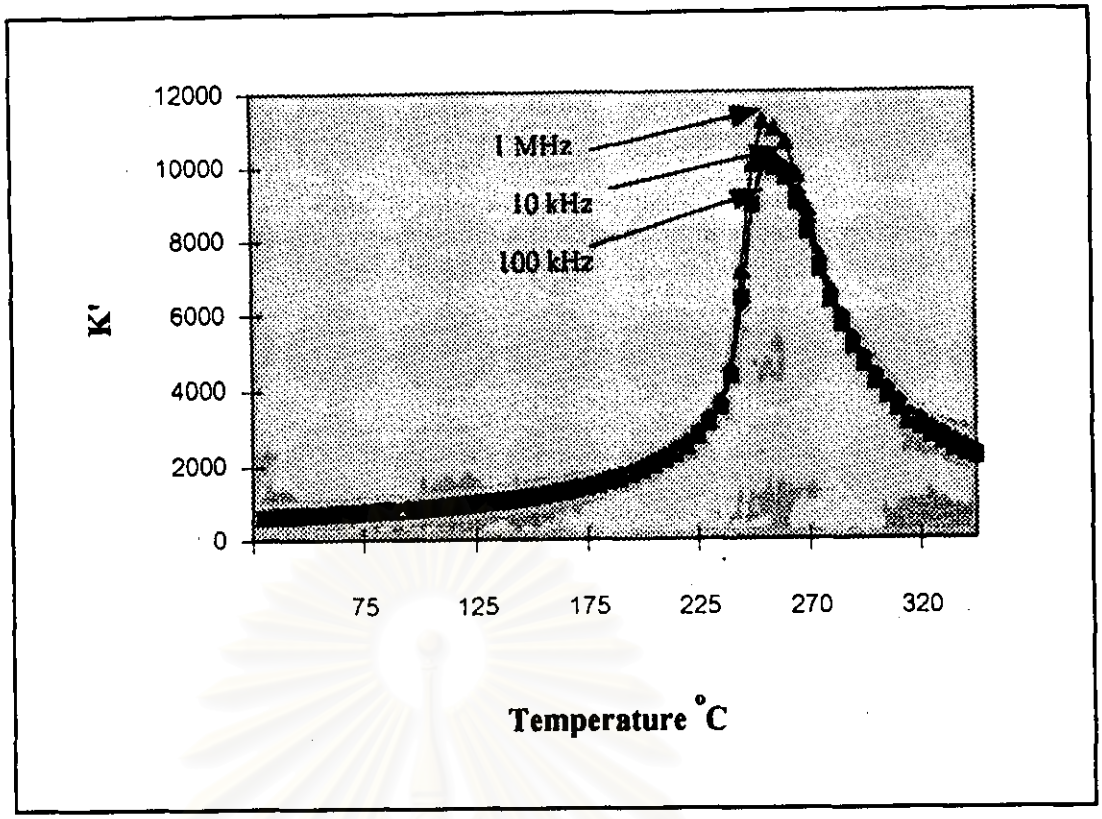

Fig.44 Temperature dependence of the dielectric constant vs frequencies for PL15T sintered at 1200°C for 2 hrs

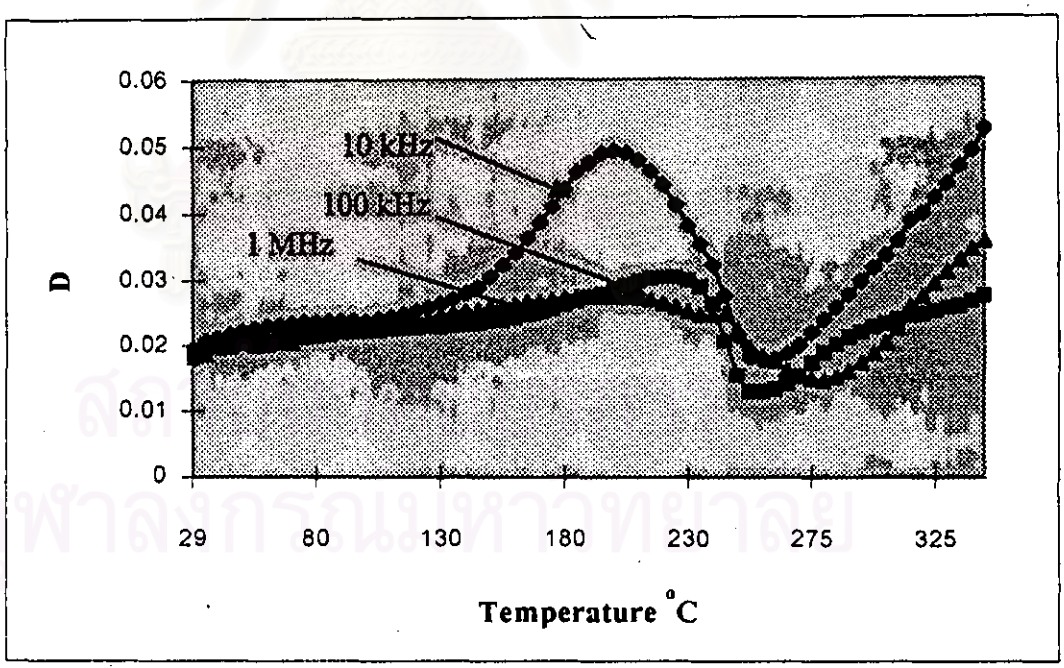

Fig. 45 Temperature dependence of the dielectric loss (D) vs frequencies for PL15T sintered at 1200°C for 2 hrs

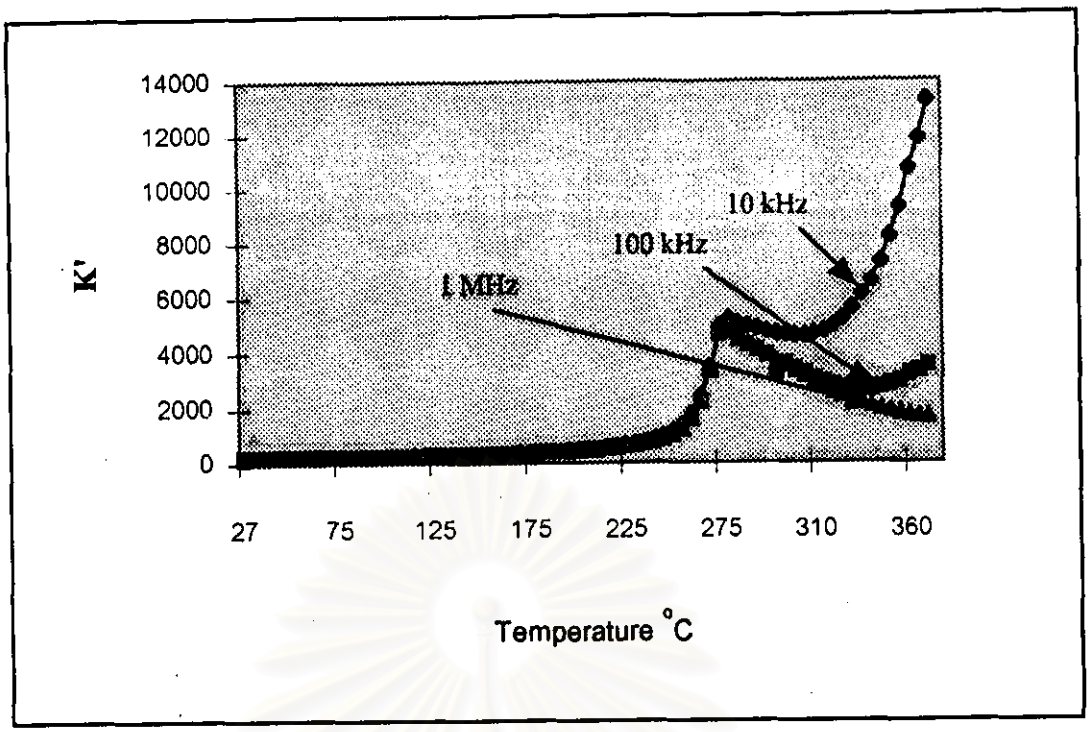

Fig.46 Temperature dependence of the dielectric constant (K') vs frequencies for PC15T sintered at 1200°C for 2 hrs

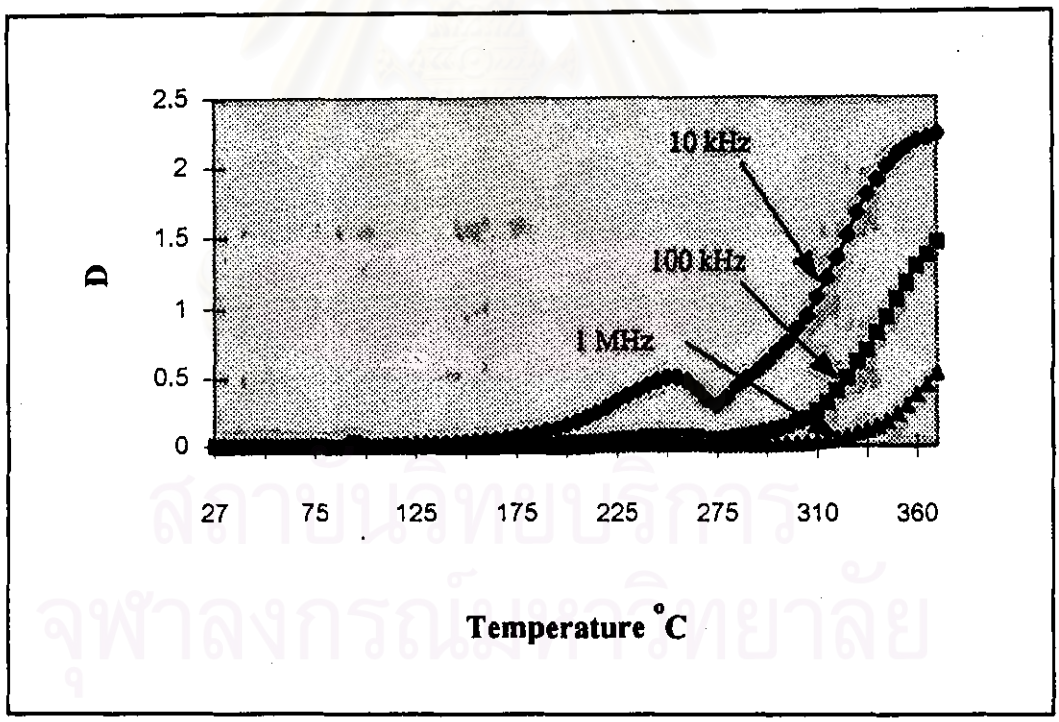

Fig.47 Temperature dependence of the dielectric loss (D) vs frequencies for PC15T sintered at 1200°C for 2 hrs

4.7 Polarization electric field (P-E)

The P-E hysteresis loop were obtained using a Virtual ground mode measuring at a frequency of 60 Hz. The applied ac field was 35 kV/cm.

All samples studied for PLT and PCT exhibited ferroelectric characteristics in form of the P-E hysteresis loops in fig. 48-51 and 55-58.

For PLT compositions, the P-E hysteresis loops of PL5T, PL10T, PL15T, and PL20T are shown in fig. 48-51, respectively.

Hysteresis measurements for PL5T and PL10T yielded elliptical curves, a characteristic of a lossy capacitor (see fig. 48 and 49). A loop for PL15T showed a characteristic of nonlinear ferroelectric with a relatively high coercive field; this may be classed as a hard ferroelectric (see fig. 50). The reversal of nonlinear ferroelectric curve was obtained for PL20T composition as shown in fig. 51. The result was not yet understood. When the resistivity measurement of PL20T composition was performed, its value was very low as compared to other than PLT compositions studied. The resistivity value of PL20T was in the range of 10^{9}-10^{11} (Ω.cm) whereas other PLT ceramics were up to 10^{14}(Ω.cm) . Low resistivity results may be attributed to have more conductive characteristic for PL20T composition.

Fig. 52 shows a tendency of increasing the remanent polarization , P_r, of PLT as a concentration of La^{3+} increases. The values of P_r increased from 3.3 to 5.7 and 25.3 $\mu C/cm^2$ for PT doped with 5%, 10%and 15%La^{3+}. However, doped

with 20%La^{3+} the remanent polarization of this composition extremely high. This is possibly caused by a lower resistivity of this composition.

Coercive field (E_c) of PLT composition increased with increasing La^{3+} concentration. E_c values increased from ~17.19 kV/cm for PL5T up to ~24.57 kV/cm for PL15T , whilst (see fig. 53) the E_c values of PL20T was 10.20 kV/cm which was lower than those of PLT compositions. It can be noted that increasing La^{3+} content to some level may lead to increasing conductivity in the PLT sample e.g. PL20T.

However, it can be noted that these results studied were not agreed with those of previous research [49] because their E_c values decreased with increasing La^{3+} concentration. This may result from the different chemical formulas of the composition, $Pb_{1-3/2x}La_xTiO_3$ as compared to $Pb_{1-x}La_xTi_{1-x/4}O_3$. In their works, the vacancies of Pb were considered on La^{3+}-doped-PT but, for this thesis, the vacancies of Ti were concentrated since their values of bulk density were more reliable. More than 100% theoretical density of $Pb_{1-3/2x}La_xTiO_3$ was reported.

The P-E hysteresis loop of PC15T and PC20T in fig. 54 and 55 showed elliptical curve, as a characteristic of a lossy capacitor. P_r and E_c values decreased from PC15T to PC20T. Typical P-E hysteresis behavior of PC30T was nearly linear dielectric with a P_r value of ~0.23 $\mu C/cm^2$ and an E_c value of ~8.58 kV/cm as seen in fig. 56. These lower values of remanent polarization, P_r and coercive field may be due to decreasing tetragonality of PCT unit cell.

The remanent polarizations , P_r of PCT composition are depicted in fig, 57. The P_r values decreased with increasing Ca^{2+} content. P_r values increased

from 2.02 $\mu C/cm^2$ for PC15T to 0.23 $\mu C/cm^2$ for PC30T. The decreasing trend of P_r may be attributed to decrease in tetragonality (c/a ratio) of the $PbTiO_3$ unit cell. However, the P_r values were lower than those of PCT thin films due to defect presented, leading to very poor in mechanical properties; for example there were many pores inside grains and grain boundary and cracking along the grain boundary. Large grain sizes may result in difficult switching domains and high internal stress.

The coercive field, E_c of PCT composition studied showed decreasing trend with increasing Ca^{2+} content as shown in fig. 58.

The remanent polarization, coercive field and dielectric properties of PLT and PCT were summarized in table 12 and 13. The trends of remanent polarization (P_r) , dielectric constant (K') and dielectric loss (D) of both PLT and PCT compositions are different. The PLT compositions showed the increasing trend whilst the PCT compositions resulted in decreasing trend. The PLT compositions gave higher values of P_r and K' than those of PCT compositions. These higher values may have been caused by La^{3+} donor additive. The difference in value with in samples studied was estimated to standard deviation values so as to the comparative results. Ca^{2+} additive would improve sintering property somewhat similar effect of calcium additive on properties of $PbTiO_3$ reported by Tien and Carlson[65].

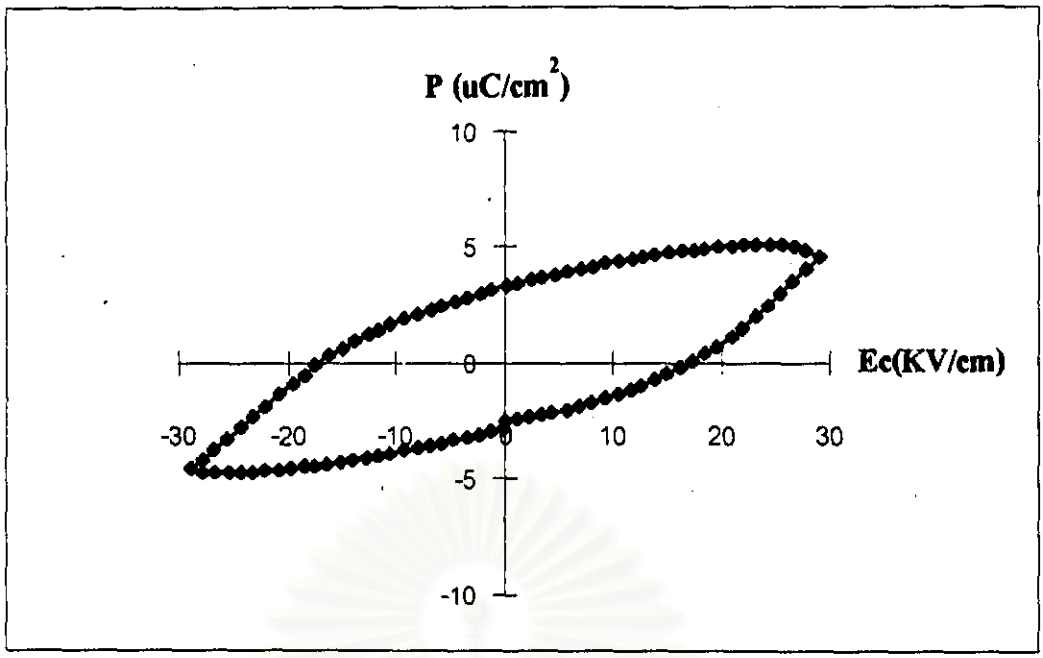

Fig.48 P-E hysteresis loop of PL5T composition sintered at 1200°C for 2 hrs measured at 35 kV / cm at room temperature

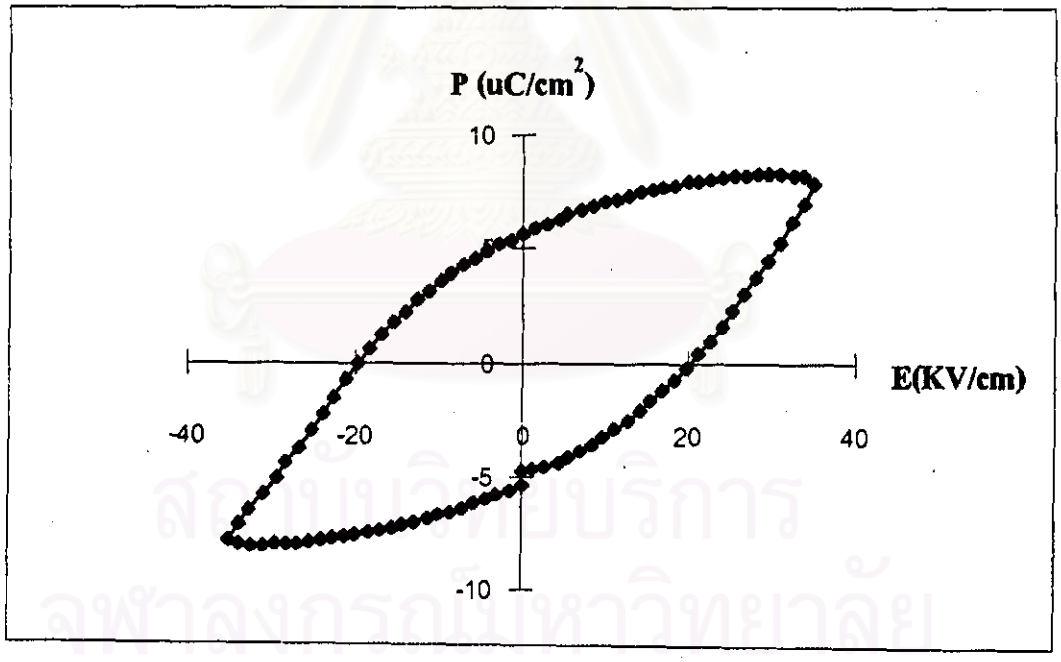

Fig. 49 P-E hysteresis loop of PL10T composition sintered at 1200°C for 2 hrs measured at 35 kV / cm at room temperature

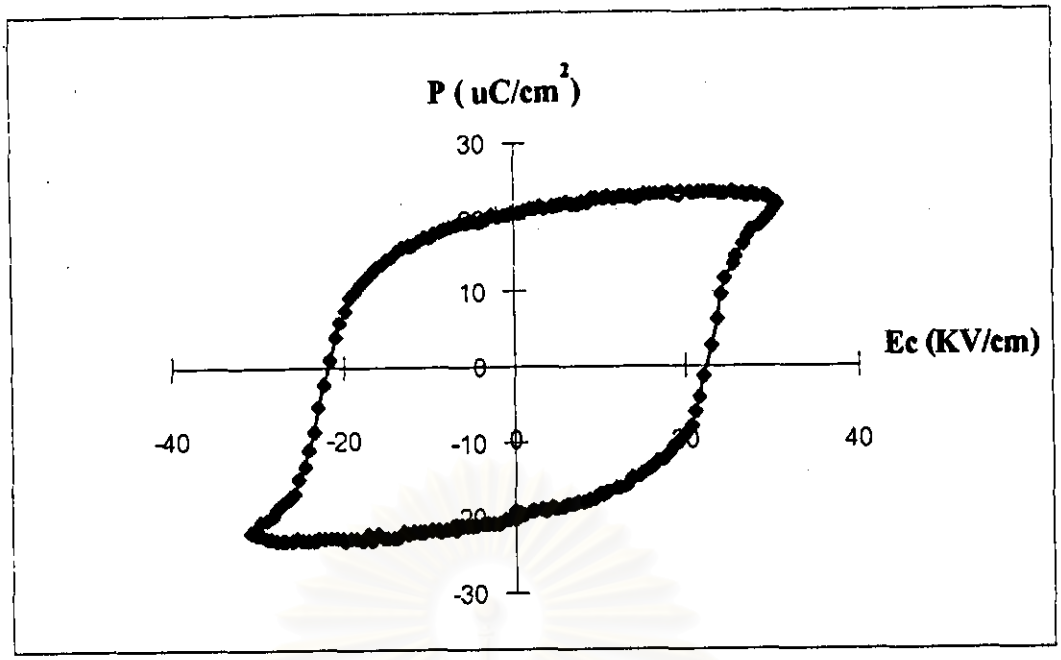

Fig. 50 P-E hysteresis loop of PL15T composition sintered at 1200°C for 2 hrs measured at 35 kV / cm at room temperature

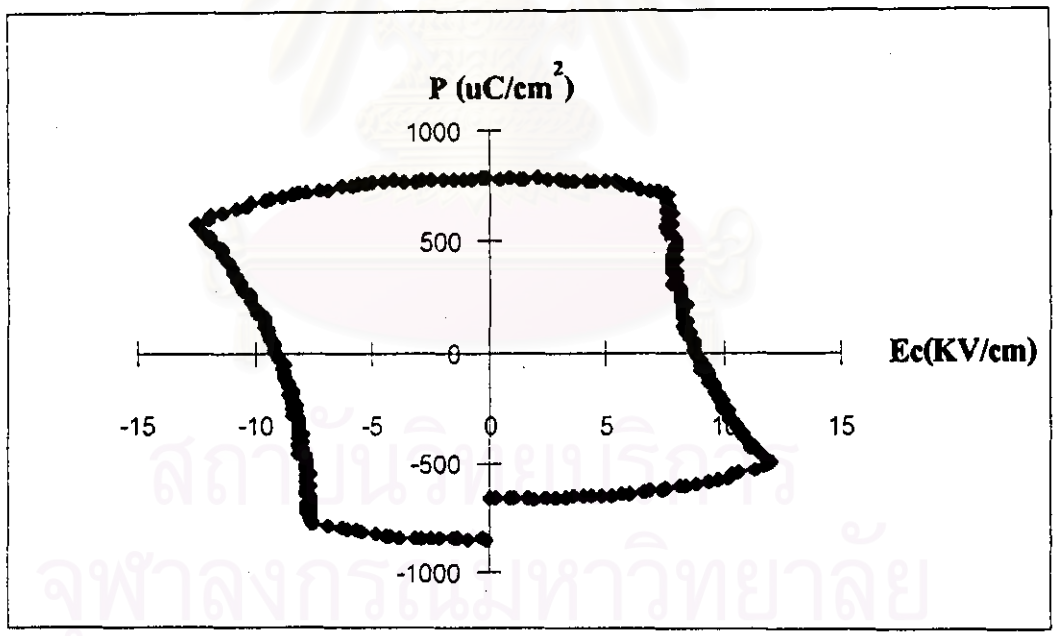

Fig. 51 P-E hysteresis loop of PL20T composition sintered at 1200°C for 2 hrs measured at 35 kV / cm at room temperature

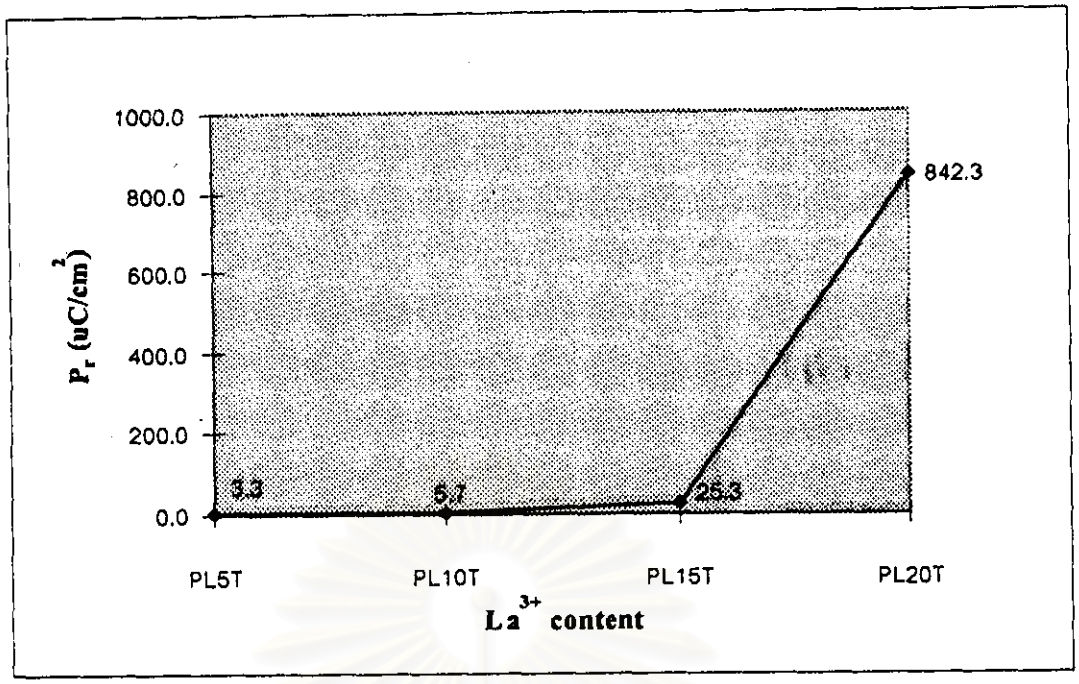

Fig. 52 Variation in remanent polarization (P_r) as a function of La^{3+} content for $Pb_{1-x}La_xTi_{1-x/4}O_3$ specimens (measured at an applied field of 35 kV/cm at room temperature)

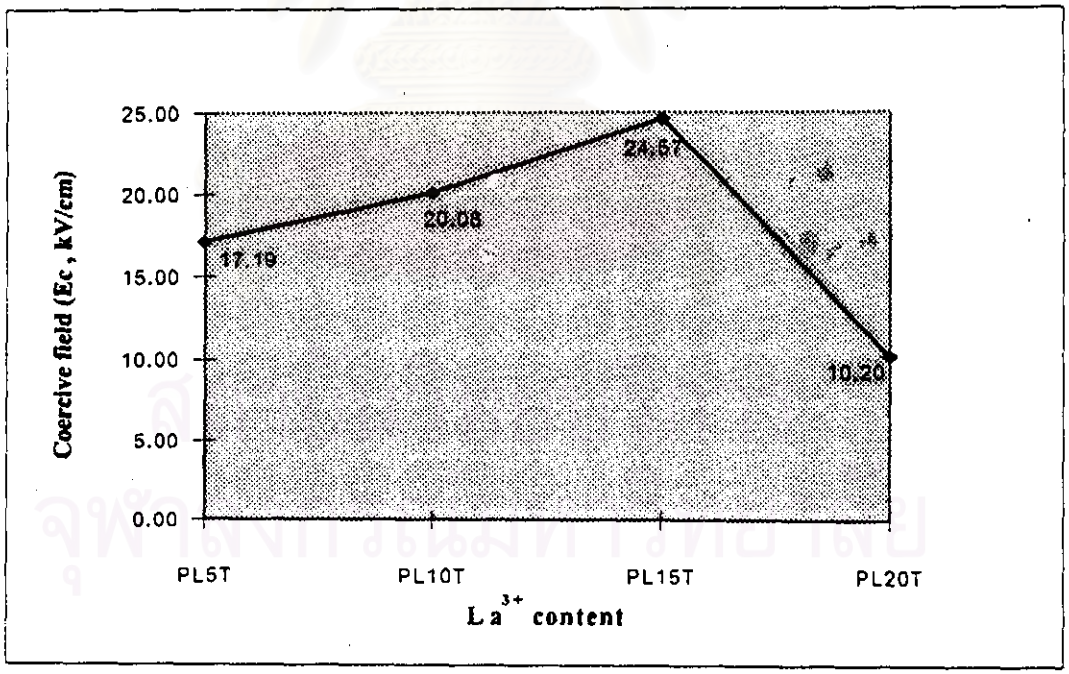

Fig. 53 Variation in coercive field (E_c), as a function of La^{3+} content for $Pb_{1-x}La_xTi_{1-x/4}O_3$ specimens (measured at an applied field of 35 kV/cm at room temperature)

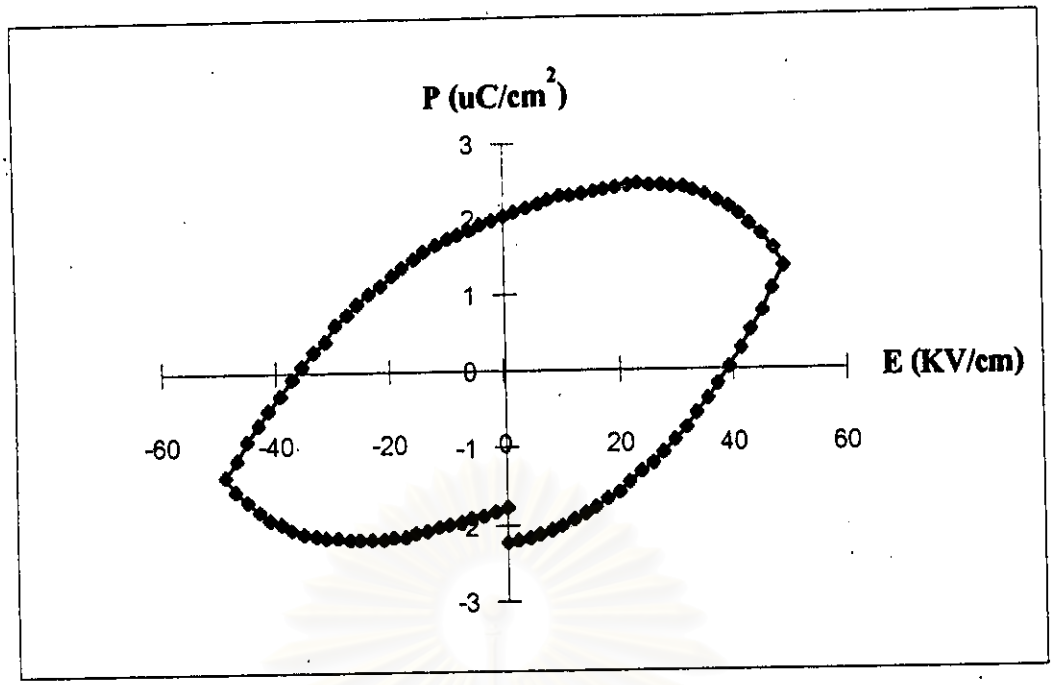

Fig. 54 P-E hysteresis loop of PC15T composition sintered at 1200°C for 2 hrs measured at 35 kV / cm at room temperature

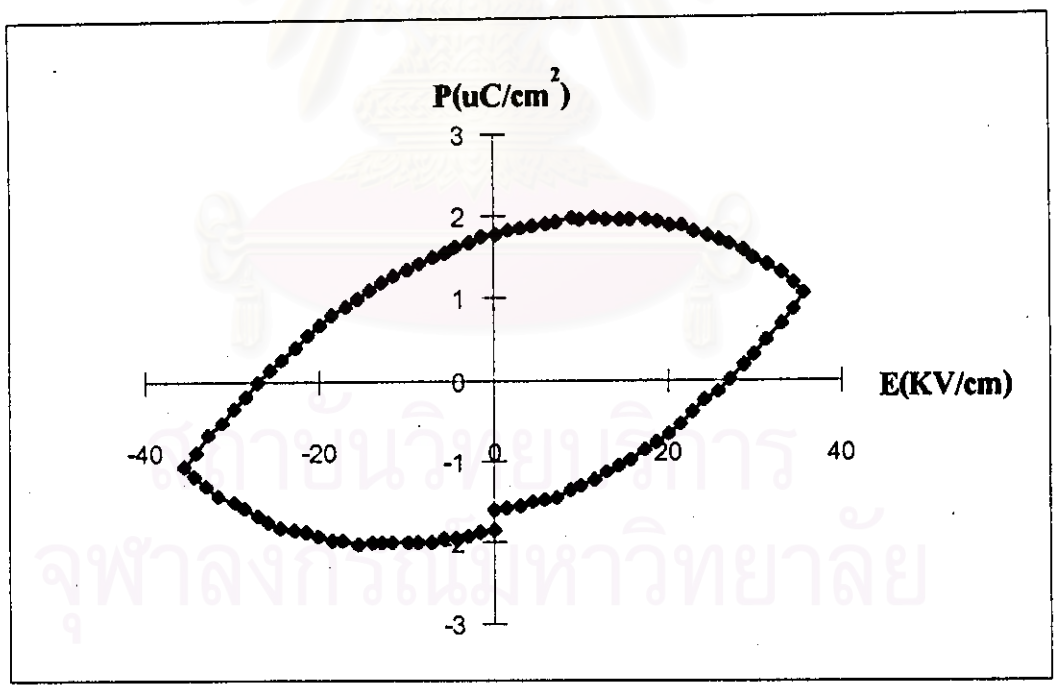

Fig. 55 P-E hysteresis loop of PC20T composition sintered at 1200°C for 2 hrs measured at 35 kV / cm at room temperature

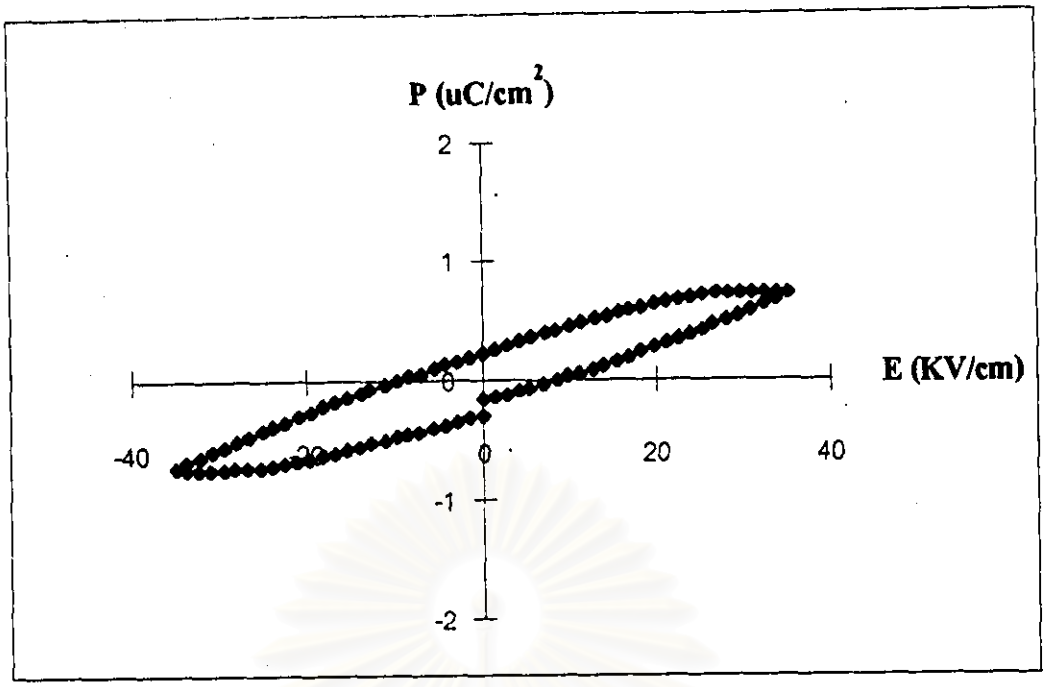

Fig. 56 P-E hysteresis loop of PC30T composition sintered at 1200°C for 2 hrs measured at 35 kV / cm at room temperature

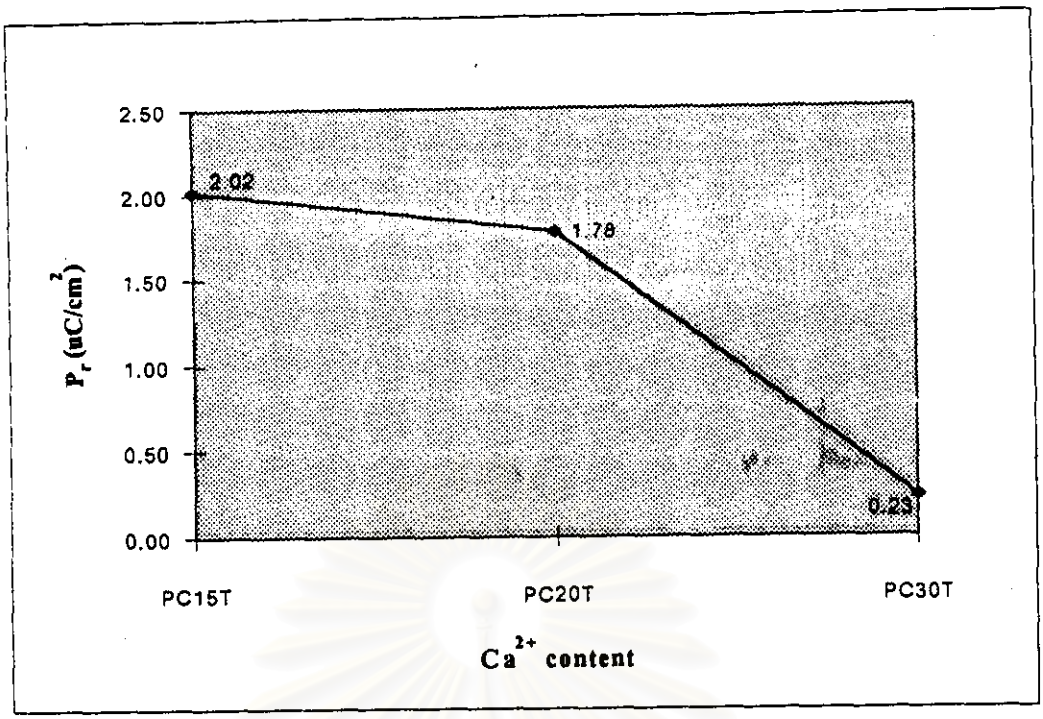

Fig. 57 Variation in remanent polarization (P_r), as a function of Ca^{2+} content for $Pb_{1-x}Ca_xTiO_3$ specimens (measured at an applied field of 35 kV/cm at room temperature)

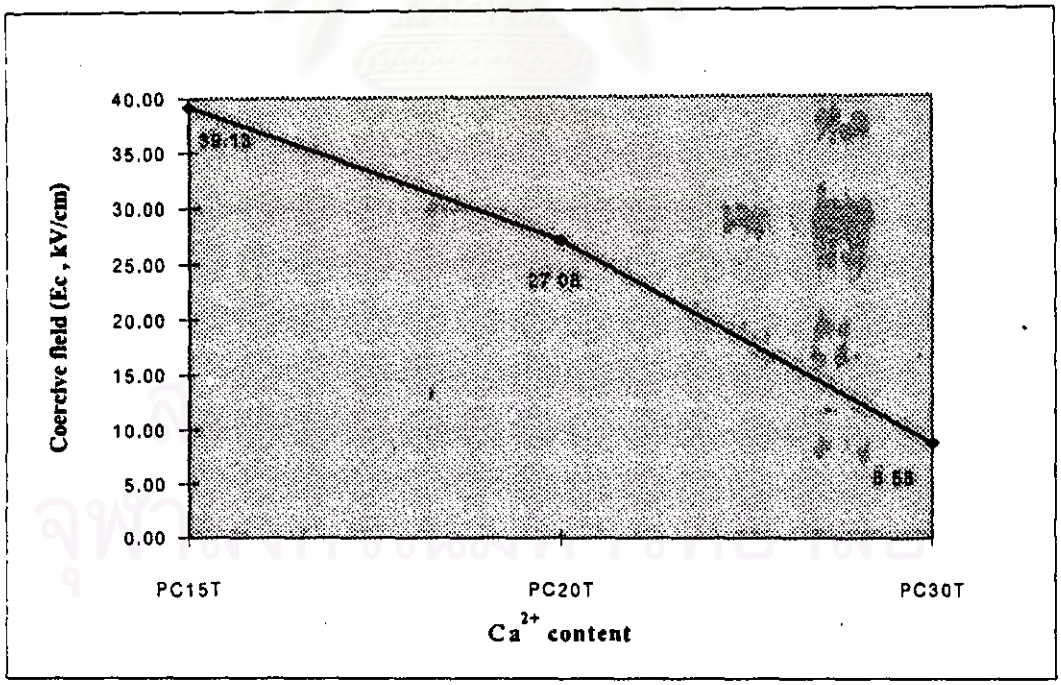

Fig. 58 Variation in coercive field (E_c), as a function of Ca^{2+} content for $Pb_{1-x}Ca_xTiO_3$ specimens (measured at an applied field of 35 kV/cm at room temperature)

Table 15 A summary of the average remanent polarization (P_r) , Coercive field (E_c) measured at 35 kV/cm. , dielectric constant (K') , dielectric loss (D) measured at a frequency of 1 kHz , and Curie temperature (T_c) of $Pb_{1-x}La_xTi_{1-x/4}O_3$ specimens sintered at 1200°C for 2 hrs

Composition	P_r ($\mu C/cm^2$)	E_c (kV/cm)	(K') @ 1 kHz (± S.D.)	(D) @ 1 kHz (± S.D.)	T_c (°C)
PL5T	3.3	17.19	412 (± 15.3)	0.050 (± 0.006)	-
PL10T	5.7	20.08	494 (± 0.47)	0.061 (± 0.009)	-
PL15T	25.3	24.57	603 (± 12.16)	0.049 (± 0.006)	255
PL20T	842.3	10.20	1281 (± 98.6)	0.578 (± 0.11)	-

Table 16 A summary of the average remanent polarization (P_r) , Coercive field (E_c) measured at 35 kV/cm. , dielectric constant (K') , dielectric loss (D) at a frequency of 1 kHz , and Curie temperature (T_c) (S.D. = standard deviation) of $Pb_{1-x}Ca_xTiO_3$ specimens sintered at 1200°C for 2 hrs

Composition	P_r ($\mu C/cm^2$) (± S.D.)	E_c (kV/cm) @ 1 kHz (± S.D.)	(K') @ 1 kHz (± S.D.)	(D) @ 1 kHz (± S.D.)	T_c (°C)
PC15T	2.02	39.13	258	1.207	280
	(± 0.25)	(± 2.5)	(± 12.3)	(± 0.09)	
PC20T	1.78	27.08	135	0.582	-
	(± 0.02)	(± 2.12)	(± 4.2)	(± 0.024)	
PC30T	0.23	8.58	192	0.066	-
	(± 0.17)	(± 3.81)	(± 6.5)	(± 0.002)	

4.8 General discussion

A primary aim of the thesis was to produce good bulk ceramics of PCT and PLT compositions. Experimentally mixed oxide technique exhibited difficulty of homogeneous solid solution. However problems were encountered for higher concentration of La and Ca ions substitution for Pb ions, whilst the high temperature calcination was taken account of high PbO vaporization and composition stoichiometry may not be attainable. Thus partial success was achieved in the preparation of PLT samples as low as 5%mole La content and PCT samples with minimum 15%mole Ca content. Since PLT compositions studies were based on chemical formula $Pb_{1-x}La_xTi_{1-x/4}O_3$, the Pb deficiency was obtained. However thin film prepared using this chemical formula resulted in better electrical properties as compared to stoichiometric $Pb_{1-x}La_xTi_{1-x/4}O_3$ compositions. In contrast, $Pb_{1-x}La_xTi_{1-x/4}O_3$ bulk ceramics exhibited values of P_r and E_c somewhat lower than those obtained from thin film samples.

Both PC15T and PC20T compositions showed many pores existing in grain and grain boundary. A very large grain size of 50-100 μm for PC15T and 5-100 μm for PC20T compositions were obtained in combination to cracking along the grain boundaries. Microstructure of PC30T compositions showed less amount of pores and smaller grain sizes of 2-200 μm. Lower P_r and E_c values may be attributed to their structure approaching to paraelectric cubic structure.

Other researcher[36] could not prepare the composition of $Pb_{1-x}Ca_xTiO_3$ ceramics where $x < 0.20$ because samples would disintergrate during cooling through the Curie point.

As the higher P_r value of PL20T composition compared to other PLT compositions was obtained and lower resistivity (10^9-10^{11} Ω.cm) was detected. This can be suggested that increasing La^{3+} content larger than 20mole% would lead to increasing conductivity property.

However, considerable more work would be required on PLT and PCT processing, characterization of the electrical properties to optimize the processing variable and the desired properties; it is essential to avoid cracking formation and obtain homogeneous solid solution.